Received 27 May 2025 Accepted 30 October 2025

DOI: 10.48308/CMCMA.4.2.38 AMS Subject Classification: 35R11

Time and Space Fractional BBM and BBM-Burgers Equations: A Semi-analytical Study Using the Shehu Transformation Adomian Decomposition Method

Sarita Pippal^{a,*}, Divyanshu Dev^b and Amandeep Singh^c

This study investigates the timefractional BenjaminBonaMahony (BBM) equation and the timespace fractional BenjaminBonaMahonyBurgers (BBMB) equation, which model nonlinear wave propagation and dispersive transport phenomena in complex media exhibiting memory and nonlocal effects. To obtain efficient analytical approximations, the Shehu Transform Adomian Decomposition Method (STADM), a novel hybrid framework that combines the Shehu Transform (ST) with the Adomian Decomposition Method (ADM), is employed to derive series-form analytical solutions for both models. A four-term series approximation is obtained for each equation, and its convergence is verified through direct comparison with the corresponding exact analytical solution. The results exhibit excellent agreement, particularly as the fractional order approaches unity $(\alpha \to 1)$, confirming the reliability and high accuracy of the proposed method. The influence of time and space fractional orders on the dynamic behavior of the solutions is analyzed through comprehensive 3D plots, which illustrate the effect of fractional parameters on wave dispersion and propagation. The main contributions of this work are: (i) the first systematic application of the STADM framework to the timespace fractional BBM and BBMB equations; (ii) the derivation of rapidly convergent analytical series solutions validated against exact results; and (iii) the demonstration of how fractional parameters modulate physical wave and diffusion processes. The proposed approach provides a simple, accurate, and computationally efficient tool for solving nonlinear fractional models relevant to wave evolution, pollutant dispersion, and oil-spill diffusion in coastal and environmental systems. Copyright © 2025 Shahid Beheshti University.

Keywords: Adomian Polynomials (AP); Shehu Transformation; BBM equation; BBM-Burger (BBMB) equation; Fractional Calculus.

Evolution differential equations (EDEs), which may include both ordinary and partial differential equations, describe the time evolution of a system. These equations play a crucial role in modeling time-dependent processes across various fields such as biology, engineering, and physics. When nonlinear terms are included, they become nonlinear evolution differential equations (NLEDEs), which can capture complex behaviors such as turbulence, chaotic dynamics, and pattern formation. Recent studies indicate that many physical, chemical, and biological systems are governed by nonlinear partial differential equations (NLPDEs) of fractional or non-integer order [33]. Over the past few decades, significant progress has been made in developing techniques to obtain exact and approximate solutions of such fractional-order NLEDEs.

Surface wave dynamics are often described by NLPDEs such as the BenjaminBonaMahony (BBM) equation, the SawadaKotera (SK) equation, the BenjaminBonaMahonyBurgers (BBMB) equation, and the Kortewegde Vries (KdV) equation, each capturing different aspects of nonlinear wave propagation. For instance, the KdV equation models wave motion in shallow water but exhibits limitations for waves with small wavenumbers, corresponding to long wavelengths. To overcome these limitations, the BenjaminBonaMahony (BBM) equation was introduced in 1972 by Benjamin, providing an improved description of long, small-amplitude waves in shallow water and other dispersive media [8]:

$$\mathcal{V}_t(x,t) + \delta_1 \mathcal{V}_x(x,t) + \delta_2 \mathcal{V} \mathcal{V}_x(x,t) - \delta_3 \mathcal{V}_{xxt}(x,t) = 0, \tag{1}$$

^a Department of Mathematics, Panjab University, Chandigarh, India.

^bDepartment of Mathematics and Scientific Computing, NIT, Hamirpur, Himachal Pradesh, India.

^c Department of Mathematics, Panjab University, Chandigarh, India.

^{*} Correspondence to: S. Pippal. Email: saritamath@pu.ac.in

where δ_1 , δ_2 , and δ_3 are constant parameters representing, respectively, the linear advection, nonlinear, and dispersive effects in the system. The coefficient δ_1 governs the wave propagation speed, δ_2 controls the strength of the nonlinear interaction responsible for wave steepening, and δ_3 accounts for dispersion, which balances nonlinearity and enables the formation of stable solitary waves. Together, these parameters determine the balance between nonlinearity and dispersion in the evolution of the wave profile.

This equation, known as the BenjaminBonaMahony (BBM) equation, is a modification of the Kortewegde Vries (KdV) equation,

$$\mathcal{V}_t(x,t) + \mathcal{V}_x(x,t) + \mathcal{V}\mathcal{V}_x(x,t) + \mathcal{V}_{xxx}(x,t) = 0, \tag{2}$$

used for (1+1)-dimensional modeling of long waves with small amplitudes. In hydrodynamics laboratories, shorter wavelength waves are often observed during wave generation experiments. Consequently, researchers have investigated various forms of the BBM equation and applied different analytical and numerical techniques to derive their solutions, as summarized below. Several authors [14, 43, 44, 46, 32, 42, 11] have considered the generalized BenjaminBonaMahony (gBBM) equation.

$$\mathcal{V}_t(x,t) + \delta_1 \mathcal{V}_x(x,t) + \delta_2 \mathcal{V}^n \mathcal{V}_x(x,t) - \delta_3 \mathcal{V}_{xxt}(x,t) = 0, \qquad n \ge 1.$$
 (3)

- For n = 1, the above equation reduces to the BenjaminBonaMahony (BBM) equation, commonly referred to as the regularized long-wave equation.
- For n=2, it simplifies to the modified BBM (mBBM) equation, which can be regarded as an analogue of the modified Kortewegde Vries (mKdV) equation:

$$\mathcal{V}_t(x,t) + \mathcal{V}_x(x,t) + \mathcal{V}^2 \mathcal{V}_x(x,t) + \mathcal{V}_{xxx}(x,t) = 0. \tag{4}$$

The BBM and modified BBM (mBBM) equations can be reduced to ordinary differential equations that are integrable in terms of elliptic functions [43] and are known to possess the Painlev property [14]. Various analytical approaches have been developed to derive traveling-wave solutions of the generalized BBM equation, including the *tanhsech* method [43, 44], the *sinecosine* method [43, 44, 46], and balancing-principle-based techniques yielding explicit solutions in terms of elliptic functions [32]. Additional methods include extended algebraic and symbolic computation approaches [42], as well as several direct approaches for obtaining traveling-wave solutions [47, 27, 18, 26]. Furthermore, semi-analytical methods such as the homotopy perturbation method (HPM) have been employed by various researchers to explore approximate solutions [21].

Many researchers, such as Yan and Biswas [47, 10], have considered the BBM equation with dual-power law nonlinearity, which can be written as

$$\mathcal{V}_t(x,t) + \delta_1 \mathcal{V}_x(x,t) + \left(\delta_2 \mathcal{V}^n + \delta_3 \mathcal{V}^{2n}\right) \mathcal{V}_x(x,t) + \delta_4 \mathcal{V}_{xxt}(x,t) = 0. \tag{5}$$

In the above equation, the first term represents the evolution term, while δ_2 and δ_3 denote the coefficients of dual-power law nonlinearity. Similarly, δ_1 and δ_4 are the coefficients associated with dispersion. The parameter n is the power-law index, and $\mathcal V$ denotes the wave profile. The exact solution of this equation for n=1 was obtained by Johnpillai *et al.* [22].

Traditionally, the study of the BBM equation has focused on integer-order derivatives. However, extending it to the fractional domain enhances its applicability for modeling wave propagation in complex media such as shallow water systems, viscoelastic materials, and stratified fluids. The fractional approach effectively captures memory effects and nonlocal interactions [13, 23, 36]. The equation has significant applications in coastal engineering for understanding wave dynamics and in geophysical fluid dynamics for analyzing oceanic and atmospheric waves. Furthermore, it plays an important role in nonlinear optics, particularly in describing pulse propagation within optical fibers. Its utility also extends to the analysis of viscoelastic materials, contributing to seismic wave modeling and stress analysis.

In this context, Kolebaje and Popoola [24] presented the fractional form of the BBM differential equation as:

$$\mathcal{V}_{t}^{\alpha}(x,t) + \mathcal{V}_{x}^{\beta}(x,t) + \mathcal{V}\mathcal{V}_{x}^{\beta}(x,t) - \mathcal{V}_{t}^{\alpha}(x,t)\mathcal{V}_{xx}^{\beta}(x,t) = 0, \tag{6}$$

and solved it using the $\frac{G}{G'}$ -expansion method. The introduction of fractional derivatives allows for a more realistic representation of physical phenomena in fluid dynamics, optics, and viscoelastic materials. These analytical approaches provide valuable insights into applications ranging from oceanic wave modeling to optical pulse propagation. Consequently, many researchers have investigated this equation using various techniques, such as the extended trial equation method [29], the fractional sub-equation method [49, 20, 45], and the generalized fractional sub-equation approach [41].

As discussed earlier, the BBM equation is a nonlinear partial differential equation that describes unidirectional wave propagation in shallow water. It incorporates nonlinearity and dispersion but does not account for dissipative effects. The BenjaminBonaMahonyBurgers (BBMB) equation is an extension of the BBM equation that describes the propagation of surface water waves in a channel [12]. It includes a damping term to model dissipative effects and can be written as:

$$\mathcal{V}_t(x,t) + \delta_1 \mathcal{V}_x(x,t) + \delta_2 \mathcal{V}^n \mathcal{V}_x(x,t) - \delta_3 \mathcal{V}_{xxt}(x,t) - \delta_4 \mathcal{V}_{xx}(x,t) = 0, \qquad n \ge 1. \tag{7}$$

- For $\delta_3 = 0$ and n = 1, the equation reduces to the Burgers equation, which describes wave propagation in acoustics and hydrodynamics.
- ullet For $\delta_4=0$, it becomes the generalized BBM (gBBM) equation.

The fractional form of the BBMB equation can be expressed as

$$\mathcal{V}_{t}^{\alpha}(x,t) + \delta_{1}\mathcal{V}_{x}^{\beta}(x,t) + \delta_{2}\mathcal{V}^{n}\mathcal{V}_{x}^{\beta}(x,t) - \delta_{3}\mathcal{V}_{t}^{\alpha}(x,t)\mathcal{V}_{xx}^{2\beta}(x,t) - \delta_{4}\mathcal{V}_{xx}^{2\beta}(x,t) = 0, \qquad n \ge 1.$$
 (8)

The BBMB and fractional BBMB equations have been solved by many researchers using analytical and semi-analytical techniques, such as the extended trial equation method [19], the fractional homotopy analysis transform method (FHATM) [25], the (G'/G)-expansion method [40], the optimal homotopy asymptotic method (OHAM) [9], the new iteration method (NIM) [34], and the Adomian decomposition method (ADM) [16].

Integral transforms are powerful tools for solving differential equations [39], as they convert complex differential problems into simpler algebraic forms. Several transformssuch as the Laplace and Sumudu transformshave been widely applied to nonlinear fractional differential equations (FDEs). Recently, Maitama and Zhao [28] introduced the Shehu transform (ST), a generalization of both the Laplace and Sumudu transforms, which has been effectively applied to a wide range of nonlinear ordinary and partial differential equations. Belgacem *et al.* [7] introduced the Shehu transform for solving Caputo-fractional differential equations and demonstrated its efficiency and simplicity compared to other integral transforms. Subsequent studies have confirmed the effectiveness of the ST in solving fractional-order differential equations. The Shehu transform has also been combined with various analytical methods, such as the NIM [5] and ADM [37, 48]. In particular, Poltem and Srimongkol [37], along with Yisa and Baruwa [48], developed the Shehu Transform Adomian Decomposition Method (STADM) to solve linear and nonlinear integral as well as integro-differential equations. A review of the literature reveals that the Shehu transform, when combined with ADM, has been effectively employed for both integer- and fractional-order differential equations [37, 48].

As fractional modeling gains traction, the fractional BBM and BBMB equations have been studied extensively. For example, Pavani *et al.* [35] derived solitary wave solutions for the time-fractional BBMBurgers equation using the Natural Transform Decomposition Method (NTDM), comparing Caputo, CaputoFabrizio, and AtanganaBaleanu derivatives. Nazneen *et al.* [31] applied the New Iterative Transform Method (NTIM) to fractional BBM/Burgers equations and demonstrated superior convergence compared to ADM, HPM, and VHPM. Abdelfattah *et al.* [2] proposed a quadrature-based solution for the fractional BBMBurgers equation, useful in tsunami modeling. Ray *et al.* [38] explored both numerical and analytical approaches for the fractional BBMBurgers equation using a reproducing kernel framework.

Research in integral transform theory has also expanded: Mlaiki *et al.* [30] established duality relations between the Shehu transform and classical transforms (Laplace, Sumudu, Fourier, etc.), facilitating hybrid transform applications in fractional PDEs. Deepak *et al.* [15] utilized a double Shehu transform to obtain exact solutions of the time-fractional wave equation, demonstrating strong computational efficiency.

Given this backdrop, the present work aims to employ the **Shehu Transform Adomian Decomposition Method (STADM)** specifically for BBM and BBMB equations with spacetime fractional derivatives. The key contributions of this approach include: (i) substituting traditional Laplace transforms (as used by Dhaigude *et al.* [16]) with the Shehu transform, and (ii) combining it with ADM to achieve faster convergence and improved handling of memory effects. Through this hybrid method, we aim to broaden the analytical toolbox for fractional wave modeling and provide accurate, computationally efficient solutions in complex media

1. Preliminaries

Definition 1.1 (Fractional Calculus and Shehu Transform Framework) Let $f:[t_0,t]\to\mathbb{R}$ be sufficiently smooth and let $0<\alpha<1$. We recall below the standard fractional derivatives and the Shehu transform family that will be used throughout this work.

1. Riemann-Liouville (R-L) fractional derivative [23, 36]:

$${}^{\rm RL}D_t^{\alpha}f(t) = \frac{1}{\Gamma(1-\alpha)} \frac{d}{dt} \int_{t_0}^t \frac{f(\tau)}{(t-\tau)^{\alpha}} d\tau. \tag{9}$$

2. Caputo fractional derivative [23, 36]:

$${}^{\mathsf{C}}D_t^{\alpha}f(t) = \frac{1}{\Gamma(1-\alpha)} \int_{t_0}^t \frac{f'(\tau)}{(t-\tau)^{\alpha}} d\tau. \tag{10}$$

The Caputo formulation permits classical (integer-order) initial conditions and is thus preferred in applied dynamical systems and fractional biological models.

3. Relation between R–L and Caputo derivatives: For $f \in C^1[t_0, t]$, the two are related by

$${}^{\mathsf{C}}D_t^{\alpha}f(t) = {}^{\mathsf{RL}}D_t^{\alpha}[f(t) - f(t_0)], \qquad 0 < \alpha < 1, \tag{11}$$

which implies that both reduce to the classical derivative df/dt as $\alpha \to 1^-$.

4. **Shehu Transform (ST)** [39]: An integral transform that generalizes both the Laplace and Sumudu transforms. Define the admissible set

$$\mathcal{Y} = \left\{ y(t) : \exists M, k_1, k_2 > 0 \text{ such that } |y(t)| < Me^{\frac{|t|}{k_i}}, \ t \in (-1)^i \times [0, \infty) \right\}.$$
 (12)

For $\mathcal{F}(t) \in \mathcal{Y}$, the Shehu Transform is

$$S[\mathcal{F}(t)] = F(s, u) = \int_0^\infty \mathcal{F}(t)e^{-\frac{st}{u}} dt, \tag{13}$$

which reduces to:

- the Laplace transform when u = 1,
- the Sumudu transform when s = 1.

Thus, it provides a unified framework with enhanced convergence properties for fractional models.

5. Inverse Shehu Transform (IST): The inverse operation reconstructs $\mathcal{F}(t)$ from F(s,u) as

$$S^{-1}[F(s,u)] = \mathcal{F}(t), \qquad t \ge 0, \tag{14}$$

with the complex inversion formula

$$\mathcal{F}(t) = \frac{1}{2\pi i} \int_{\alpha - i\infty}^{\alpha + i\infty} \frac{1}{u} e^{\frac{st}{u}} F(s, u) \, ds, \tag{15}$$

where the contour of integration lies along $\Re(s) = \alpha$, chosen to ensure convergence.

6. Shehu Transform of the Caputo fractional derivative: For $\beta > 0$, the Shehu Transform of ${}^{C}D_{t}^{\beta}V(x,t)$ is given by [1, 6]

$$\mathcal{S}\left[{}^{C}D_{t}^{\beta}\mathcal{V}(x,t)\right] = \left(\frac{s}{u}\right)^{\beta}V(x,s,u) - \sum_{j=0}^{m-1}\left(\frac{s}{u}\right)^{\beta-j-1}\frac{\partial^{j}\mathcal{V}(x,t)}{\partial t^{j}}\bigg|_{t=0}.$$
 (16)

Remark 1.2 (On the choice of fractional derivative) In this study, the Caputo fractional derivative is employed because it allows the use of physically meaningful integer-order initial and boundary conditions. Unlike the Riemann–Liouville derivative, the Caputo operator ensures that the derivative of a constant is zero and maintains compatibility with experimentally measurable quantities. While the Atangana–Baleanu derivative incorporates a non-singular kernel suitable for systems with long-term memory effects, it is less convenient for analytical computations. For a detailed comparison of these operators and their physical relevance, Hence, the Caputo definition is adopted here for its analytical simplicity and physical interpretability.

2. Proposed Algorithm for the Solution of the Fractional BBM-Burgers Equation

For a detailed discussion of the Shehu Transform Adomian Decomposition Method (STADM), the reader is referred to our recent publication [17] and references therein. That work presents foundational concepts, mathematical structure, and utility for fractional partial differential equations (FPDEs). In this paper, we employ the STADM to solve the fractional Benjamin–Bona–Mahony–Burgers (BBMB) equation in both temporal and spatial fractional domains.

The general form of the space-time fractional BBMB equation is given by

$$\frac{\partial^{\alpha} \mathcal{V}(x,t)}{\partial t^{\alpha}} + \frac{\partial^{\beta} \mathcal{V}(x,t)}{\partial x^{\beta}} + \mathcal{V}^{m}(x,t) \frac{\partial^{\beta} \mathcal{V}(x,t)}{\partial x^{\beta}} - \frac{\partial^{2\beta} \mathcal{V}(x,t)}{\partial x^{2\beta}} - \frac{\partial^{2\beta}}{\partial x^{2\beta}} \left(\frac{\partial^{\alpha} \mathcal{V}(x,t)}{\partial t^{\alpha}} \right) = 0, \tag{17}$$

where $0 < \alpha, \beta < 1$, $m \ge 1$, and the initial condition is

$$\mathcal{V}(x,0) = f(x). \tag{18}$$

Applying the Shehu Transform (ST) defined in Eq. (13) to Eq. (17) and using the property for the Caputo derivative (Eq. (16)) yields

$$\mathcal{S}\left[\frac{\partial^{\alpha} \mathcal{V}}{\partial t^{\alpha}}\right] = -\mathcal{S}\left[\frac{\partial^{\beta} \mathcal{V}}{\partial x^{\beta}}\right] - \mathcal{S}\left[\mathcal{V}^{m}\frac{\partial^{\beta} \mathcal{V}}{\partial x^{\beta}}\right] + \mathcal{S}\left[\frac{\partial^{2\beta} \mathcal{V}}{\partial x^{2\beta}}\right] + \mathcal{S}\left[\frac{\partial^{2\beta} \mathcal{V}}{\partial x^{2\beta}}\left(\frac{\partial^{\alpha} \mathcal{V}}{\partial t^{\alpha}}\right)\right]. \tag{19}$$

Using Eq. (16), Eq. (19) can be written in transform variables (s, u) as :

$$\left(\frac{s}{u}\right)^{\alpha}V(x,s,u) - \left(\frac{s}{u}\right)^{\alpha-1}V(x,0) = -\mathcal{S}\left[\frac{\partial^{\beta}V}{\partial x^{\beta}}\right] - \mathcal{S}\left[V^{m}\frac{\partial^{\beta}V}{\partial x^{\beta}}\right] + \mathcal{S}\left[\frac{\partial^{2\beta}V}{\partial x^{2\beta}}\right] + \mathcal{S}\left[\frac{\partial^{2\beta}V}{\partial x^{2\beta}}\right].$$
(20)

Solving Eq. (20) for V(x, s, u) gives :

$$V(x,s,u) = \left(\frac{u}{s}\right)\mathcal{V}(x,0) - \left(\frac{u}{s}\right)^{\alpha}\mathcal{S}\left[\frac{\partial^{\beta}\mathcal{V}}{\partial x^{\beta}}\right] - \left(\frac{u}{s}\right)^{\alpha}\mathcal{S}\left[\mathcal{V}^{m}\frac{\partial^{\beta}\mathcal{V}}{\partial x^{\beta}}\right] + \left(\frac{u}{s}\right)^{\alpha}\mathcal{S}\left[\frac{\partial^{2\beta}\mathcal{V}}{\partial x^{2\beta}}\right] + \mathcal{S}\left[\frac{\partial^{2\beta}\mathcal{V}}{\partial x^{2\beta}}\right]. \tag{21}$$

Applying the Inverse Shehu Transform (IST), Eq. (14), to Eq. (21) yields :

$$\mathcal{V}(x,t) = f(x) - \mathcal{S}^{-1} \left[\left(\frac{u}{s} \right)^{\alpha} \mathcal{S}[\mathcal{L}^{1}] \right] - \mathcal{S}^{-1} \left[\left(\frac{u}{s} \right)^{\alpha} \mathcal{S}[\mathcal{N}] \right] + \mathcal{S}^{-1} \left[\left(\frac{u}{s} \right)^{\alpha} \mathcal{S}[\mathcal{L}^{2}] \right] + \mathcal{S}^{-1} \left[\left(\frac{u}{s} \right)^{\alpha} \mathcal{S}[\mathcal{L}^{3}] \right], \tag{22}$$

where \mathcal{L}^1 , \mathcal{L}^2 , and \mathcal{L}^3 denote the linear terms, and \mathcal{N} represents the nonlinear term. Now assume a series representation for the solution:

$$\mathcal{V}(x,t) = \sum_{k=0}^{\infty} \mathcal{V}_k(x,t), \tag{23}$$

with the initial term

$$\mathcal{V}_0(x,t) = f(x),\tag{24}$$

and the recurrence relation for higher-order terms ($k \ge 1$) given by

$$\mathcal{V}_{k}(x,t) = -\mathcal{S}^{-1}\left[\left(\frac{u}{s}\right)^{\alpha}\mathcal{S}[\mathcal{L}_{(k-1)}^{1}]\right] - \mathcal{S}^{-1}\left[\left(\frac{u}{s}\right)^{\alpha}\mathcal{S}[\mathcal{A}_{(k-1)}]\right] + \mathcal{S}^{-1}\left[\left(\frac{u}{s}\right)^{\alpha}\mathcal{S}[\mathcal{L}_{(k-1)}^{2}]\right] + \mathcal{S}^{-1}\left[\left(\frac{u}{s}\right)^{\alpha}\mathcal{S}[\mathcal{L}_{(k-1)}^{3}]\right], \quad (25)$$

where $\mathcal{A}_{(k-1)}$ are the Adomian polynomials (AP) [3, 4] representing the nonlinear term $\mathcal{N}.$

This complete formulation constitutes the **Shehu Transform Adomian Decomposition Method (STADM)** for solving the fractional BBM–Burgers equation. In general, the Adomian polynomials (AP) for the nonlinear term $\mathcal N$ are calculated as follows:

$$\mathcal{A}_0 = \mathcal{V}_0^m \frac{\partial^6 \mathcal{V}_0}{\partial \mathbf{v}^6}, \tag{26}$$

$$\mathcal{A}_{1} = \frac{\partial}{\partial \lambda} \left[(\mathcal{V}_{0} + \lambda \mathcal{V}_{1})^{m} \frac{\partial^{\beta}}{\partial x^{\beta}} (\mathcal{V}_{0} + \lambda \mathcal{V}_{1}) \right] \Big|_{\lambda=0} = \mathcal{V}_{0}^{m} \frac{\partial^{\beta} \mathcal{V}_{1}}{\partial x^{\beta}} + m \mathcal{V}_{0}^{m-1} \mathcal{V}_{1} \frac{\partial^{\beta} \mathcal{V}_{0}}{\partial x^{\beta}}, \tag{27}$$

$$\mathcal{A}_{2} = \frac{1}{2!} \frac{\partial^{2}}{\partial \lambda^{2}} \left[(\mathcal{V}_{0} + \lambda \mathcal{V}_{1} + \lambda^{2} \mathcal{V}_{2})^{m} \frac{\partial^{\beta}}{\partial x^{\beta}} (\mathcal{V}_{0} + \lambda \mathcal{V}_{1} + \lambda^{2} \mathcal{V}_{2}) \right]_{\lambda=0}$$
(28)

$$= \frac{1}{2!} \left[2 \mathcal{V}_0^m \frac{\partial^{\beta} \mathcal{V}_2}{\partial x^{\beta}} + m \mathcal{V}_0^{m-1} \mathcal{V}_1 \frac{\partial^{\beta} \mathcal{V}_1}{\partial x^{\beta}} + m \mathcal{V}_0^{m-1} \mathcal{V}_1 \frac{\partial^{\beta} \mathcal{V}_1}{\partial x^{\beta}} + m (m-1) \mathcal{V}_0^{m-2} \mathcal{V}_1^2 \frac{\partial^{\beta} \mathcal{V}_0}{\partial x^{\beta}} \right], \tag{29}$$

$$\vdots = \vdots$$
 (30)

$$\mathcal{A}_k = \frac{1}{k!} \frac{d^k}{d\lambda^k} \mathcal{N} \left(\sum_{j=0}^k \lambda^j \mathcal{V}_j \right) \bigg|_{\lambda=0}, \quad k \geq 0,$$

where, in the case of the nonlinear term $\mathcal{N} = \mathcal{V}^m \frac{\partial^{\beta} \mathcal{V}}{\partial x^{\beta}}$, this expression represents the decomposition of the nonlinear operator applied to the series sum of components \mathcal{V}_i .

2.1. Convergence and Error Analysis

To validate the reliability and numerical accuracy of the proposed **Shehu Transform Adomian Decomposition Method (STADM)**, we examined the convergence behavior and error characteristics of the obtained series solutions for the time–fractional and time–space fractional BBM/BBMB equations. The convergence of the STADM series solution is represented as:

$$\mathcal{V}(x,t) = \sum_{n=0}^{\infty} \mathcal{V}_n(x,t),$$

where each term $V_n(x,t)$ is recursively generated using the Shehu Transform and Adomian polynomial components. In practice, we observed that a four-term partial sum,

$$V_4(x, t) = V_0 + V_1 + V_2 + V_3$$

is sufficient to ensure strong convergence across the considered fractional order range $(0.5 \le \alpha, \beta \le 1)$.

To quantify the approximation accuracy, we computed the *absolute error* between the approximate and exact analytical solutions as:

$$E(x, t) = |\mathcal{V}_{\text{exact}}(x, t) - \mathcal{V}_{\text{approx}}(x, t)|.$$

Additionally, the following global error norms were evaluated:

MaxErr = max
$$|E(x, t)|$$
, $L_2 = \sqrt{\sum_{i=1}^{N} (E_i)^2}$, RMS = $\sqrt{\frac{1}{N} \sum_{i=1}^{N} (E_i)^2}$,

where N denotes the number of spatial discretization points, the results reveal that the error decreases rapidly with successive series terms, exhibiting a geometric-like convergence pattern. For higher fractional orders ($\alpha, \beta \geq 0.6$), the MaxErr, L_2 , and RMS values become very small, confirming the high accuracy of the STADM approximation. Moreover, as the fractional parameters approach unity ($\alpha, \beta \to 1$), the approximate series solution smoothly converges to the classical integer-order analytical solution. This quantitative validation demonstrates that the STADM framework provides a numerically stable and highly accurate approach compared with standard transform-based decomposition methods, effectively capturing both local and nonlocal fractional dynamics.

3. Implementation of the Proposed Algorithm on Numerical Examples

3.1. **Example 1**

Consider the following time-fractional BBM equation, whose exact solution is $\alpha=1$ is ${\rm sech}^2\left(\frac{x}{4}-\frac{t}{4}\right)$:

$${}^{\alpha}\mathcal{V}_{t}(x,t) + \mathcal{V}_{x}(x,t) + \mathcal{V}\mathcal{V}_{x}(x,t) - \mathcal{V}_{xxt}(x,t) = 0, \quad 0 < \alpha \le 1.$$

$$(31)$$

with the initial condition $V(x, 0) = \operatorname{sech}^2\left(\frac{x}{4}\right)$.

Applying the ST and then IST to the above equation, and using the initial condition, the solution can be written as:

$$\mathcal{V} = \mathcal{V}_0 - \mathcal{S}^{-1} \left[\left(\frac{u}{s} \right)^{\alpha} \mathcal{S} \left[\mathcal{V}_x(x,t) \right] \right] - \mathcal{S}^{-1} \left[\left(\frac{u}{s} \right)^{\alpha} \mathcal{S} \left[\mathcal{V} \mathcal{V}_x(x,t) \right] \right] + \mathcal{S}^{-1} \left[\left(\frac{u}{s} \right)^{\alpha} \mathcal{S} \left[\mathcal{V}_{xxt}(x,t) \right] \right]. \tag{32}$$

Or, more succinctly:

$$\mathcal{V} = \mathcal{V}_0 - \mathcal{S}^{-1} \left[\left(\frac{u}{s} \right)^{\alpha} \mathcal{S}[\mathcal{L}^1] \right] - \mathcal{S}^{-1} \left[\left(\frac{u}{s} \right)^{\alpha} \mathcal{S}[\mathcal{N}] \right] + \mathcal{S}^{-1} \left[\left(\frac{u}{s} \right)^{\alpha} \mathcal{S}[L^2] \right], \tag{33}$$

where \mathbf{L}^1 and \mathbf{L}^2 are linear terms of the equation, while \mathbf{N} is the nonlinear term . Also, take the first trem of sereis as the initial condition:

$$\mathcal{V}_0 = \mathcal{V}(x,0) = \operatorname{sech}^2\left(\frac{x}{4}\right).$$

The remaining terms of the series can be found using the recurrence relation

$$\sum_{i=1}^{\infty} \mathcal{V}_{i} = -\mathcal{S}^{-1} \left[\left(\frac{u}{s} \right)^{\alpha} \mathcal{S} \left[\sum_{i=1}^{\infty} \mathsf{L}_{(i-1)}^{1} \right] \right] - \mathcal{S}^{-1} \left[\left(\frac{u}{s} \right)^{\alpha} \mathcal{S} \left[\sum_{i=1}^{\infty} \mathsf{N}_{(i-1)} \right] \right] + \mathcal{S}^{-1} \left[\left(\frac{u}{s} \right)^{\alpha} \mathcal{S} \left[\sum_{i=1}^{\infty} \mathsf{L}_{(i-1)}^{2} \right] \right]. \tag{34}$$

Here, Adomian polynomials (AP) are used to decompose the nonlinear term. Successive terms can be explicitly computed as:

$$\begin{array}{lll} \mathcal{V}_{1} & = & -\mathcal{S}^{-1}\left[\left(\frac{u}{s}\right)^{\alpha}\mathcal{S}[\mathsf{L}_{0}^{1}]\right] - \mathcal{S}^{-1}\left[\left(\frac{u}{s}\right)^{\alpha}\mathcal{S}[\mathsf{N}_{0}]\right] + \mathcal{S}^{-1}\left[\left(\frac{u}{s}\right)^{\alpha}\mathcal{S}[\mathsf{L}_{0}^{2}]\right] \\ & = & -\mathcal{S}^{-1}\left[\left(\frac{u}{s}\right)^{\alpha}\mathcal{S}[(\mathcal{V}_{0})_{x}]\right] - \mathcal{S}^{-1}\left[\left(\frac{u}{s}\right)^{\alpha}\mathcal{S}[\mathcal{A}_{0}]\right] + \mathcal{S}^{-1}\left[\left(\frac{u}{s}\right)^{\alpha}\mathcal{S}[(\mathcal{V}_{0})_{xxt}]\right], \\ \mathcal{A}_{0} & = & \mathcal{V}_{0}\frac{\partial\mathcal{V}_{0}}{\partial x} = -\frac{1}{2}\mathrm{sech}^{4}\left(\frac{x}{4}\right)\tan\left(\frac{x}{4}\right) = f_{0}(x), \\ \mathcal{V}_{1} & = & \frac{t^{\alpha}}{\Gamma(\alpha+1)}\frac{\sinh\left(\frac{x}{4}\right)\left[\cosh^{2}\left(\frac{x}{4}\right) + 1\right]}{2\cosh^{5}\left(\frac{x}{4}\right)} = \frac{t^{\alpha}}{\Gamma(\alpha+1)}f_{1}(x). \end{array}$$

Similarly,

$$\begin{array}{lll} \mathcal{V}_2 & = & -\mathcal{S}^{-1}\left[\left(\frac{u}{s}\right)^\alpha \mathcal{S}[\mathsf{L}_1^1]\right] - \mathcal{S}^{-1}\left[\left(\frac{u}{s}\right)^\alpha \mathcal{S}[\mathsf{N}_1]\right] + \mathcal{S}^{-1}\left[\left(\frac{u}{s}\right)^\alpha \mathcal{S}[\mathsf{L}_1^2]\right] \\ & = & -\mathcal{S}^{-1}\left[\left(\frac{u}{s}\right)^\alpha \mathcal{S}\left[\frac{\partial \mathcal{V}_1}{\partial x}\right]\right] - \mathcal{S}^{-1}\left[\left(\frac{u}{s}\right)^\alpha \mathcal{S}[\mathcal{A}_1]\right] + \mathcal{S}^{-1}\left[\left(\frac{u}{s}\right)^\alpha \mathcal{S}\left[\frac{\partial^3 \mathcal{V}_1}{\partial x^2 \partial t}\right]\right], \\ \mathcal{A}_1 & = & \mathcal{V}_0\frac{\partial \mathcal{V}_1}{\partial x} + \mathcal{V}_1\frac{\partial \mathcal{V}_0}{\partial x} = \frac{t^\alpha}{\Gamma(\alpha+1)}\frac{2-\sinh^2\frac{x}{4}(9+4\sinh^2\frac{x}{4})}{8\cosh^8\frac{x}{4}} = \frac{t^\alpha}{\Gamma(\alpha+1)}f_2(x), \\ \mathcal{V}_2 & = & -\frac{t^{2\alpha}}{\Gamma(2\alpha+1)}\left[(f_1(x))_x + f_2(x)\right] + (f_1(x))_{xx}\frac{t^{2\alpha-1}}{\Gamma(2\alpha)}. \end{array}$$

Where $(f_1(x))_x$ and $(f_1(x))_{xx}$ are given explicitly as:

$$(f_1(x))_x = \frac{2-\sinh^2\left(\frac{x}{4}\right)\left(5+2\sinh^2\left(\frac{x}{4}\right)\right)}{8\cosh^6\left(\frac{x}{4}\right)}, \qquad (f_1(x))_{xx} = \frac{2\sinh^5\left(\frac{x}{4}\right)+6\sinh^3\left(\frac{x}{4}\right)-11\sinh\left(\frac{x}{4}\right)}{16\cosh^7\left(\frac{x}{4}\right)}.$$

Likewise, higher terms such as V_3 can be found and explicitly expressed using previously computed functions and their derivatives. The full form for V_3 as well as all auxiliary $f_i(x)$ and $G_i(x)$ functions is provided for completeness.

$$\begin{split} \mathcal{V}_3 &= -\mathcal{S}^{-1} \left[\left(\frac{u}{s} \right)^\alpha \mathcal{S} \left[\mathbf{L}_2^1 \right] \right] - \mathcal{S}^{-1} \left[\left(\frac{u}{s} \right)^\alpha \mathcal{S} \left[\mathbf{N}_2 \right] \right] + \mathcal{S}^{-1} \left[\left(\frac{u}{s} \right)^\alpha \mathcal{S} \left[\mathbf{L}_2^2 \right] \right] \\ &= -\mathcal{S}^{-1} \left[\left(\frac{u}{s} \right)^\alpha \mathcal{S} \left[\frac{\partial \mathcal{V}_2}{\partial x} \right] \right] - \mathcal{S}^{-1} \left[\left(\frac{u}{s} \right)^\alpha \mathcal{S} \left[\mathcal{A}_2 \right] \right] + \mathcal{S}^{-1} \left[\left(\frac{u}{s} \right)^\alpha \mathcal{S} \left[\frac{\partial^3 \mathcal{V}_2}{\partial x^2 \partial t} \right] \right] \\ &= -\mathcal{S}^{-1} \left[\left(\frac{u}{s} \right)^\alpha \mathcal{S} \left[(f_1(x))_{xxx} \frac{t^{2\alpha - 1}}{\Gamma(2\alpha)} - \frac{t^{2\alpha}}{\Gamma(2\alpha + 1)} \left((f_1(x))_{xx} + (f_2(x))_x \right) \right] \right] - \mathcal{S}^{-1} \left[\left(\frac{u}{s} \right)^\alpha \mathcal{S} \left[\mathcal{A}_2 \right] \right] \\ &+ \mathcal{S}^{-1} \left[\left(\frac{u}{s} \right)^\alpha \mathcal{S} \left[-2\alpha \frac{t^{2\alpha - 1}}{\Gamma(2\alpha + 1)} \left((f_1(x))_{xxx} + (f_2(x))_{xx} \right) + \frac{t^{2\alpha - 2}}{\Gamma(2\alpha)} \left(f_1(x))_{xxxx} (2\alpha - 1) \right] \right] \\ &= -(f_1(x))_{xxx} \frac{t^{2\alpha - 1}}{\Gamma(3\alpha - 1)} + \left((f_1(x))_{xx} + (f_2(x))_x \right) \frac{t^{3\alpha}}{\Gamma(3\alpha)} - \mathcal{S}^{-1} \left[\left(\frac{u}{s} \right)^\alpha \mathcal{S} \left[\mathcal{A}_2 \right] \right] \\ &+ \left(f_1(x) \right)_{xxxx} \frac{t^{2\alpha}}{\Gamma(3\alpha)} - \left((f_1(x))_{xxx} + (f_2(x))_{xx} \right) \frac{t^{3\alpha - 1}}{\Gamma(3\alpha - 1)} , \\ \mathcal{S}^{-1} \left[\left(\frac{u}{s} \right)^\alpha \mathcal{S} \left[\mathcal{A}_2 \right] \right] = \mathcal{S}^{-1} \left[\left(\frac{u}{s} \right)^\alpha \mathcal{S} \left[\mathcal{V}_1 \frac{\partial \mathcal{V}_1}{\partial x} + \mathcal{V}_2 \frac{\partial \mathcal{V}_0}{\partial x} + \mathcal{V}_0 \frac{\partial \mathcal{V}_2}{\partial x} \right] \right] . \\ &= \mathcal{G}_1(x) \mathcal{S}^{-1} \left[\left(\frac{u}{s} \right)^\alpha \mathcal{S} \left[\frac{t^{2\alpha}}{(\Gamma(\alpha + 1))^2} \right] \right] + \mathcal{G}_2(x) \mathcal{S}^{-1} \left[\left(\frac{u}{s} \right)^\alpha \mathcal{S} \left[\frac{t^{2\alpha - 1}}{\Gamma(2\alpha)} \right] \right] - \mathcal{G}_3(x) \mathcal{S}^{-1} \left[\left(\frac{u}{s} \right)^\alpha \mathcal{S} \left[\frac{t^{2\alpha}}{\Gamma(1 + 2\alpha)} \right] \right] , \\ &= \mathcal{G}_1(x) \frac{t^{3\alpha} \Gamma(2\alpha + 1)}{(\Gamma(\alpha + 1))^2 \Gamma(3\alpha)} + \mathcal{G}_2(x) \frac{t^{3\alpha - 1}}{\Gamma(3\alpha - 1)} - \mathcal{G}_3(x) \frac{t^{3\alpha}}{\Gamma(3\alpha)} . \end{split}$$

Where,

$$f_{2}(x) = \frac{2 - 9 \sinh^{2}\left(\frac{x}{4}\right) - 4 \sinh^{4}\left(\frac{x}{4}\right)}{8 \cosh^{8}\left(\frac{x}{4}\right)}, f_{2}(x)_{x} = \frac{19 \sinh^{3}\left(\frac{x}{4}\right) + 8 \sinh^{5}\left(\frac{x}{4}\right) - 17 \sinh\left(\frac{x}{4}\right)}{16 \cosh^{9}\left(\frac{x}{4}\right)}, \\ f_{1}(x)_{xxxx} = \frac{32 \sinh\left(\frac{x}{4}\right) - 70 \sinh^{3}\left(\frac{x}{4}\right) + 4 \sinh^{5}\left(\frac{x}{4}\right) + \sinh^{7}\left(\frac{x}{4}\right)}{32 \cosh^{9}\left(\frac{x}{4}\right)}, f_{1}(x)_{xxx} = \frac{84 \sinh^{2}\left(\frac{x}{4}\right) - 14 \sinh^{4}\left(\frac{x}{4}\right) - 11 - 4 \sinh^{6}\left(\frac{x}{4}\right)}{64 \cosh^{8}\left(\frac{x}{4}\right)}, \\ f_{2}(x)_{xx} = \frac{193 \sinh^{2}\left(\frac{x}{4}\right) - 32 \sinh^{6}\left(\frac{x}{4}\right) - 74 \sinh^{4}\left(\frac{x}{4}\right) - 17}{64 \cosh^{10}\left(\frac{x}{4}\right)}, G_{1} = \frac{4 \sinh\left(\frac{x}{4}\right) - 9 \sinh^{9}\left(\frac{x}{4}\right) - 8 \sinh^{3}\left(\frac{x}{4}\right) - 2 \sinh^{7}\left(\frac{x}{4}\right)}{16 \cosh^{11}\left(\frac{x}{4}\right)}, \\ G_{2} = \frac{106 \sinh^{2}\left(\frac{x}{4}\right) - 11 - 26 \sinh^{4}\left(\frac{x}{4}\right) - 8 \sinh^{6}\left(\frac{x}{4}\right)}{64 \cosh^{10}\left(\frac{x}{4}\right)}, G_{3} = \frac{26 \sinh^{3}\left(\frac{x}{4}\right) + 27 \sinh^{5}\left(\frac{x}{4}\right) + 4 \sinh^{7}\left(\frac{x}{4}\right) - 32 \sinh\left(\frac{x}{4}\right)}{16 \cosh^{11}\left(\frac{x}{4}\right)}.$$

The first three terms of the series solution are given by:

$$\mathcal{V} = \sum_{i=0}^{3} \mathcal{V}_{i} = \operatorname{sech}^{2} \left(\frac{x}{4} \right) + \frac{t^{\alpha}}{\Gamma(\alpha+1)} f_{1}(x) - \frac{t^{2\alpha}}{\Gamma(2\alpha+1)} \left[(f_{1}(x))_{x} + f_{2}(x) \right] + (f_{1}(x))_{xx} \frac{t^{2\alpha-1}}{\Gamma(2\alpha)}$$

$$+ \left[(f_{1}(x))_{xx} + (f_{2}(x))_{x} + (f_{1}(x))_{xxxx} + G_{3}(x) \right] \frac{t^{3\alpha}}{\Gamma(3\alpha+1)} - G_{1}(x) \frac{t^{3\alpha}\Gamma(2\alpha+1)}{(\Gamma(\alpha+1))^{2}\Gamma(3\alpha+1)}$$

$$- \frac{t^{3\alpha-1}}{\Gamma(3\alpha)} \left[2(f_{1}(x))_{xxx} + (f_{2}(x))_{xx} + G_{2}(x) \right].$$

One potential concern is the number of terms needed for the series solution to converge effectively. To address this, **Figure 1** displays the convergence behavior of our series solution for eight distinct values of the fractional order parameter α : 0.65, 0.68, 0.7, 0.75, 0.8, 0.85, 0.9, and 1. In this analysis, the time variable t is fixed at 0.1, while α is varied to study its influence on the convergence of the series. The figure clearly shows that the series solution closely approximates the exact solution across almost all selected values of α . This indicates that, within this fractional order range, the series provides an accurate representation of the true solution. In particular, for larger values of α , the series solution nearly coincides with the exact solution, demonstrating improved approximation as α increases. This result highlights a key characteristic of the series: its convergence improves as more terms are included. The series delivers progressively better approximations with each additional term. Remarkably, in this case, including just four terms yields a solution that closely matches the exact solution, indicating sufficient convergence. While further terms may enhance accuracy, four terms are adequate to achieve the desired precision in this scenario. The convergence of the

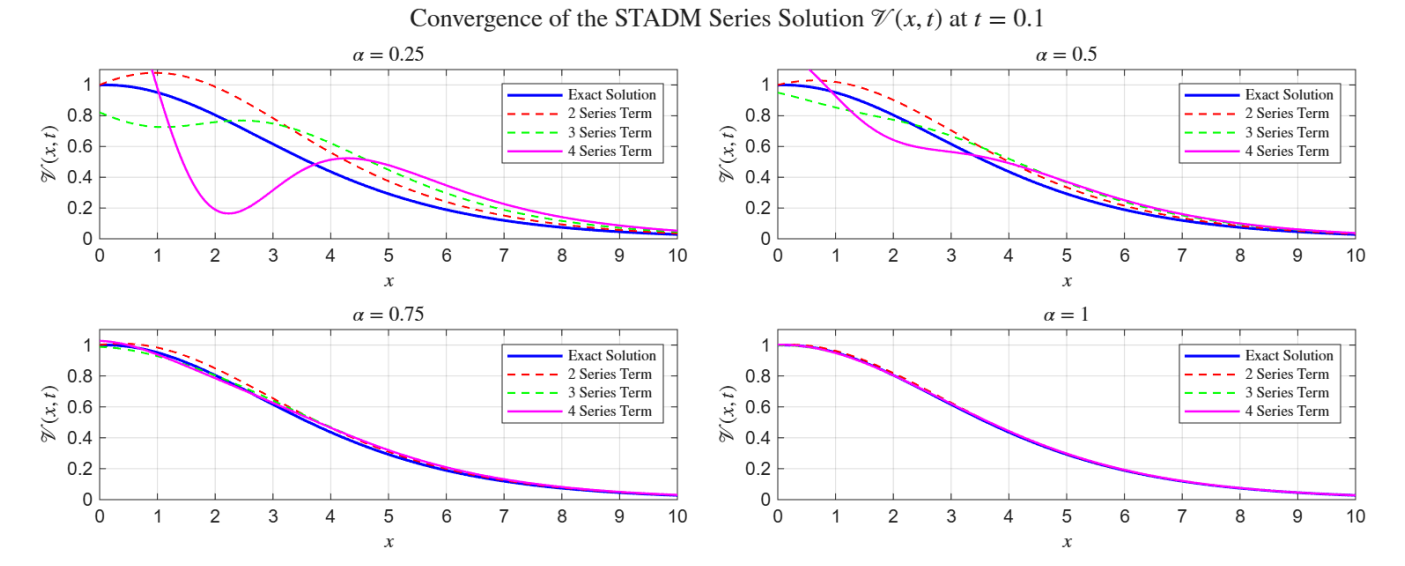


Figure 1. Converge of present solution for different series terms for Example 1.

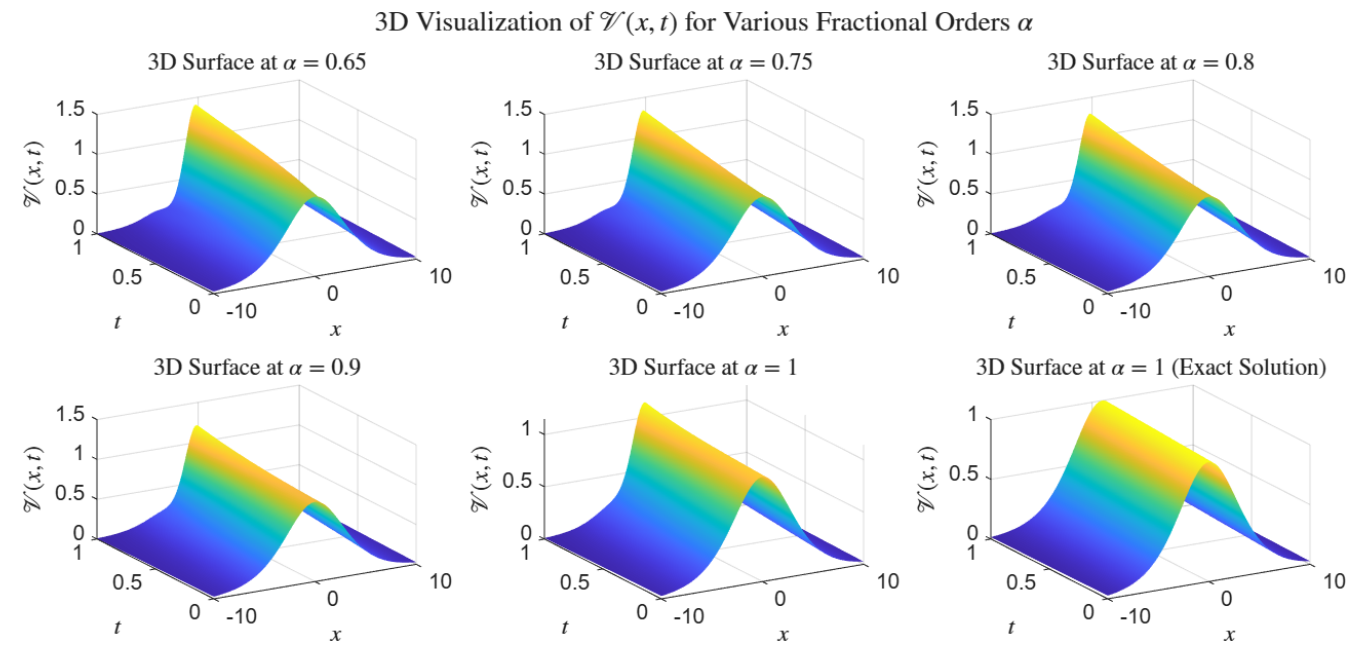


Figure 2. Influence of the fractional-order parameter α on the series solution. Three-dimensional representation of the approximate solution $\mathcal{V}(x,t)$ computed with four terms in the series expansion for $\alpha=0.7$, 0.8, 0.9, and 1.0. As α increases toward unity, the fractional-order solution converges to the classical integer-order profile, demonstrating the accuracy and convergence efficiency of the proposed method.

proposed series solution is efficiently achieved using only four terms, as illustrated in the previous figure. This indicates that the truncated series provides an accurate and computationally efficient approximation of the systems dynamics. Accordingly, Figure, 1 explores the influence of the fractional-order parameter, α , on the solution while maintaining the series expansion up to the fourth term. To investigate the impact of fractional differentiation, four representative values of α are considered: 0.7, 0.8, 0.9, and 1.0. These correspond to increasing levels of memory effect in the fractional operator, with $\alpha=1$ representing the classical integer-order model. The time variable is varied over the interval $t\in[0,1]$, and the spatial domain is defined as $x\in[-10,10]$. The results clearly demonstrate that as α approaches unity, the fractional-order solution converges smoothly toward the exact integer-order solution. This trend highlights the consistency of the fractional formulation with the classical case and confirms the accuracy of the series approach. Conversely, for smaller values of α , the solution exhibits more pronounced deviations, reflecting the nonlocal and hereditary characteristics inherent in fractional-order systems. In summary, **Figure 2** verifies that the proposed semi-analytical series method achieves rapid convergence and high accuracy with only four terms, while effectively capturing the influence of fractional dynamics across different α values.

Table f 1 quantifies the convergence behavior of the proposed STADM approach for the time-fractional BBM equation at t=0.1

Table 1. Error measures for the four-term STADM approximation of the time-fractional BBM equation at t = 0.1. The errors decrease rapidly as α increases, confirming strong convergence toward the exact analytical solution.

α	$\max E(x, t) $	$ E _{2}$	RMS
0.65	7.749×10^{-2}	1.516×10^{-1}	2.397×10^{-2}
0.68	6.052×10^{-2}	1.267×10^{-1}	2.003×10^{-2}
0.70	5.117×10^{-2}	1.127×10^{-1}	1.782×10^{-2}
0.75	3.330×10^{-2}	8.484×10^{-2}	1.341×10^{-2}
0.80	2.569×10^{-2}	6.437×10^{-2}	1.018×10^{-2}
0.85	1.990×10^{-2}	4.876×10^{-2}	7.709×10^{-3}
0.90	1.507×10^{-2}	3.634×10^{-2}	5.746×10^{-3}
1.00	7.390×10^{-3}	1.735×10^{-2}	2.743×10^{-3}

(Example 1). The maximum absolute, L^2 , and RMS errors all decrease monotonically as the fractional order α increases from 0.65 to 1.0. This demonstrates that the four-term series solution exhibits strong and stable convergence. In particular, for $\alpha \geq 0.8$, the numerical errors fall below 10^{-2} , indicating that the approximate solution nearly coincides with the exact analytical solution $\mathcal{V}_{\text{exact}}(x,t) = \text{sech}^2\left(\frac{x}{4} - \frac{t}{4}\right)$. The results confirm that the STADM provides a highly accurate and rapidly convergent semi-analytical framework for solving fractional BBM-type equations.

3.2. Example 2

Consider the time-fractional BBMB equation as:

$$\frac{\partial^{\alpha} \mathcal{V}(x,t)}{\partial t^{\alpha}} + \frac{\partial \mathcal{V}(x,t)}{\partial x} + \mathcal{V}(x,t) \frac{\partial \mathcal{V}(x,t)}{\partial x} - \frac{\partial^{2} \mathcal{V}(x,t)}{\partial x^{2}} - \frac{\partial^{2}}{\partial x^{2}} \frac{\partial^{\alpha} \mathcal{V}(x,t)}{\partial t^{\alpha}} = 0.$$
 (35)

Its operational ST form is written as:

$$\mathcal{V}(x,t) = \mathcal{V}(x,0) - \mathcal{S}^{-1} \left[\left(\frac{u}{s} \right)^{\alpha} \mathcal{S}[\mathcal{N}] \right] - \mathcal{S}^{-1} \left[\left(\frac{u}{s} \right)^{\alpha} \mathcal{S}[\mathcal{L}^{1}] \right] + \mathcal{S}^{-1} \left[\left(\frac{u}{s} \right)^{\alpha} \mathcal{S}[\mathcal{L}^{2}] \right] + \mathcal{S}^{-1} \left[\left(\frac{u}{s} \right)^{\alpha} \mathcal{S}[\mathcal{L}^{3}] \right], \tag{36}$$

where, $\mathcal{L}^1 = \mathcal{V}_x$, $\mathcal{L}^2 = \mathcal{V}_{xx}$, $\mathcal{L}^3 = \mathcal{V}_{xxt}$, represent the linear operators, and $\mathcal{N} = \mathcal{V} \mathcal{V}_x$, denotes the nonlinear term. Let the initial condition be $\mathcal{V}(x,0) = f(x) = \sin x$. Hence,

$$\mathcal{V}(x,t) = \sin x - \mathcal{S}^{-1} \left[\left(\frac{u}{s} \right)^{\alpha} \mathcal{S}[\mathcal{L}^{1}] \right] - \mathcal{S}^{-1} \left[\left(\frac{u}{s} \right)^{\alpha} \mathcal{S}[\mathcal{N}] \right] + \mathcal{S}^{-1} \left[\left(\frac{u}{s} \right)^{\alpha} \mathcal{S}[\mathcal{L}^{2}] \right] + \mathcal{S}^{-1} \left[\left(\frac{u}{s} \right)^{\alpha} \mathcal{S}[\mathcal{L}^{3}] \right]. \tag{37}$$

The nonlinear part is decomposed using Adomian polynomials (AP). The STADM series components are thus defined as:

$$\mathcal{V}_0(x,t) = \mathcal{V}(x,0) = \sin x,\tag{38}$$

$$\mathcal{V}_{1}(x,t) = -\mathcal{S}^{-1}\left[\left(\frac{u}{s}\right)^{\alpha}\mathcal{S}[\mathcal{N}_{0}]\right] - \mathcal{S}^{-1}\left[\left(\frac{u}{s}\right)^{\alpha}\mathcal{S}[\mathcal{L}_{0}^{1}]\right] + \mathcal{S}^{-1}\left[\left(\frac{u}{s}\right)^{\alpha}\mathcal{S}[\mathcal{L}_{0}^{2}]\right] + \mathcal{S}^{-1}\left[\left(\frac{u}{s}\right)^{\alpha}\mathcal{S}[\mathcal{L}_{0}^{3}]\right]. \tag{39}$$

For the zeroth iteration, the differential operators yield:

$$\mathcal{L}_0^1 = \partial_x \mathcal{V}_0 = \cos x, \qquad \mathcal{L}_0^2 = \partial_{xx} \mathcal{V}_0 = -\sin x, \qquad \mathcal{L}_0^3 = \partial_t \partial_{xx} \mathcal{V}_0 = 0, \text{ nonlinear term } \mathcal{N}_0 = \mathcal{V}_0 \ \partial_x \mathcal{V}_0 = \sin x \cos x = \frac{1}{2} \sin(2x). \tag{40}$$

Since for a time-independent function g(x),

$$S^{-1}\left[\left(\frac{u}{s}\right)^{\alpha}S[g(x)]\right] = I_t^{\alpha}g(x) = \frac{t^{\alpha}}{\Gamma(1+\alpha)}g(x),\tag{41}$$

hence, the first-order correction becomes

$$\mathcal{V}_1(x,t) = -\frac{t^{\alpha}}{\Gamma(1+\alpha)} \left[\frac{1}{2} \sin(2x) + \cos x + \sin x \right]. \tag{42}$$

Hence, the first two components of the STADM series solution are :

$$\mathcal{V}(x,t) \approx \mathcal{V}_0(x,t) + \mathcal{V}_1(x,t) = \sin x - \frac{t^{\alpha}}{\Gamma(1+\alpha)} \left[\frac{1}{2} \sin(2x) + \cos x + \sin x \right]. \tag{43}$$

Higher-order components can be obtained recursively using Eq. (37). Now, the first Adomian polynomial is defined as:

$$\mathcal{A}_0 = \mathcal{V}_0 \, \partial_x \mathcal{V}_0 = \sin x \cos x. \tag{44}$$

Hence, after taking inverse transforms, we obtain

$$\mathcal{V}_1(x,t) = -\frac{t^{\alpha}}{\Gamma(\alpha+1)} k_1(x), \quad \text{, where,} \quad k_1(x) = \sin x \cos x + \sin x + \cos x. \tag{45}$$

Proceeding to the next order, we have

$$\mathcal{V}_{2} = -\mathcal{S}^{-1} \left[\left(\frac{u}{s} \right)^{\alpha} \mathcal{S}[\mathcal{N}_{1}] \right] - \mathcal{S}^{-1} \left[\left(\frac{u}{s} \right)^{\alpha} \mathcal{S}[\mathcal{L}_{1}^{1}] \right] + \mathcal{S}^{-1} \left[\left(\frac{u}{s} \right)^{\alpha} \mathcal{S}[\mathcal{L}_{1}^{2}] \right] + \mathcal{S}^{-1} \left[\left(\frac{u}{s} \right)^{\alpha} \mathcal{S}[\mathcal{L}_{1}^{3}] \right]. \tag{46}$$

The inverse transform contributions are computed as:

$$S^{-1}\left[\left(\frac{u}{s}\right)^{\alpha}S[\mathcal{L}_{1}^{1}]\right] = -\frac{t^{2\alpha}}{\Gamma(2\alpha+1)}\left[\cos x - \sin x + \cos(2x)\right],\tag{47}$$

$$S^{-1}\left[\left(\frac{u}{s}\right)^{\alpha}S[\mathcal{L}_{1}^{2}]\right] = \frac{t^{2\alpha}}{\Gamma(2\alpha+1)}\left[\cos x + \sin x + 2\sin(2x)\right],\tag{48}$$

$$S^{-1}\left[\left(\frac{u}{s}\right)^{\alpha}S[\mathcal{L}_{1}^{3}]\right] = \frac{t^{2\alpha-1}}{\Gamma(2\alpha)}\left[\cos x + \sin x + 2\sin(2x)\right],\tag{49}$$

$$S^{-1}\left[\left(\frac{u}{s}\right)^{\alpha}S[A_1]\right] = -\frac{t^{2\alpha}}{\Gamma(2\alpha+1)}\left[\sin(2x) + \cos(2x) + \sin x(\cos(2x) + \cos^2 x)\right]. \tag{50}$$

Collecting all terms, we have :

$$V_2 = \frac{t^{2\alpha}}{\Gamma(2\alpha + 1)} k_2(x) + \frac{t^{2\alpha - 1}}{\Gamma(2\alpha)} k_3(x), \tag{51}$$

where,

$$k_2(x) = 2(\sin x + \cos x + \sin 2x + \cos 2x) - 3\sin^3 x, \quad k_3(x) = \sin x + \cos x + 2\sin 2x.$$
 (52)

For the third-order term, the recurrence relation yields

$$\mathcal{V}_{3} = -\mathcal{S}^{-1} \left[\left(\frac{u}{s} \right)^{\alpha} \mathcal{S}[\mathcal{N}_{2}] \right] - \mathcal{S}^{-1} \left[\left(\frac{u}{s} \right)^{\alpha} \mathcal{S}[\mathcal{L}_{2}^{1}] \right] + \mathcal{S}^{-1} \left[\left(\frac{u}{s} \right)^{\alpha} \mathcal{S}[\mathcal{L}_{2}^{2}] \right] + \mathcal{S}^{-1} \left[\left(\frac{u}{s} \right)^{\alpha} \mathcal{S}[\mathcal{L}_{2}^{3}] \right]. \tag{53}$$

The individual inverse transform terms are obtained as:

$$S^{-1}\left[\left(\frac{u}{s}\right)^{\alpha}S[\mathcal{L}_{2}^{1}]\right] = \frac{t^{3\alpha}}{\Gamma(3\alpha+1)}(k_{2})_{x} + \frac{t^{3\alpha-1}}{\Gamma(3\alpha)}(k_{3})_{x},\tag{54}$$

$$S^{-1}\left[\left(\frac{u}{s}\right)^{\alpha}S[\mathcal{L}_{2}^{2}]\right] = \frac{t^{3\alpha}}{\Gamma(3\alpha+1)}(k_{2})_{xx} + \frac{t^{3\alpha-1}}{\Gamma(3\alpha)}(k_{3})_{xx},\tag{55}$$

$$\mathcal{S}^{-1}\left[\left(\frac{u}{s}\right)^{\alpha}\mathcal{S}\left[\mathcal{L}_{2}^{3}\right]\right] = \frac{t^{3\alpha-1}}{\Gamma(3\alpha)}(k_{2})_{xx} + \frac{t^{3\alpha-2}}{\Gamma(3\alpha-1)}(k_{3})_{xx},\tag{56}$$

$$S^{-1}\left[\left(\frac{u}{s}\right)^{\alpha}S[\mathcal{A}_{2}]\right] = \frac{t^{3\alpha}}{\Gamma(3\alpha+1)}k_{4} + \frac{t^{3\alpha-1}}{\Gamma(3\alpha)}k_{5} + \frac{t^{3\alpha}}{\Gamma(3\alpha+1)}\left[f_{1}(f_{1})_{x}\frac{\Gamma(2\alpha+1)}{(\Gamma(\alpha+1))^{2}}\right]. \tag{57}$$

The spatial derivatives and auxiliary functions are:

$$(k_2)_x = -9\sin^2 x \cos x - 2\sin x - 4\sin 2x + 2\cos x + 4\cos 2x, (k_3)_x = -\sin x + \cos x + 4\cos 2x, (k_2)_{xx} = 9\sin^3 x - 18\sin x \cos^2 x - 2\sin x - 8\sin 2x - 2\cos x - 8\cos 2x, (k_3)_{xx} = -(\sin x + \cos x + 8\sin 2x).$$
 (58)

The additional polynomial functions are defined as:

$$k_4 = (1 + 2\sin x)(2\cos 2x - 2\sin 2x) + 2\cos x(\sin 2x + \cos 2x) - 12\sin^3 x\cos x,$$

$$k_5 = \sin 2x + \cos 2x + 2(\sin 2x\cos x + 2\cos x\sin 2x).$$
(59)

Finally, combining all terms, the third-order correction is obtained as

$$V_{3} = \frac{t^{3\alpha}}{\Gamma(3\alpha+1)} F_{1}(x) + \frac{t^{3\alpha-1}}{\Gamma(3\alpha)} F_{2}(x) + \frac{t^{3\alpha-2}}{\Gamma(3\alpha-1)} (k_{3})_{xx} - \frac{t^{3\alpha}}{\Gamma(3\alpha+1)} \Big[f_{1}(f_{1})_{x} \frac{\Gamma(2\alpha+1)}{(\Gamma(\alpha+1))^{2}} \Big], \tag{60}$$

where

$$F_1(x) = 15\cos x + 12\sin^3 x \cos x + 39\sin^3 x - 12\cos^3 x - 26\sin x - 2\sin 2x - 14\cos 2x$$

$$F_2(x) = 29\sin^3 x - 16\sin 2x - 21\sin x - 13\cos 2x - 4\cos x - 2\sin 3x.$$
(61)

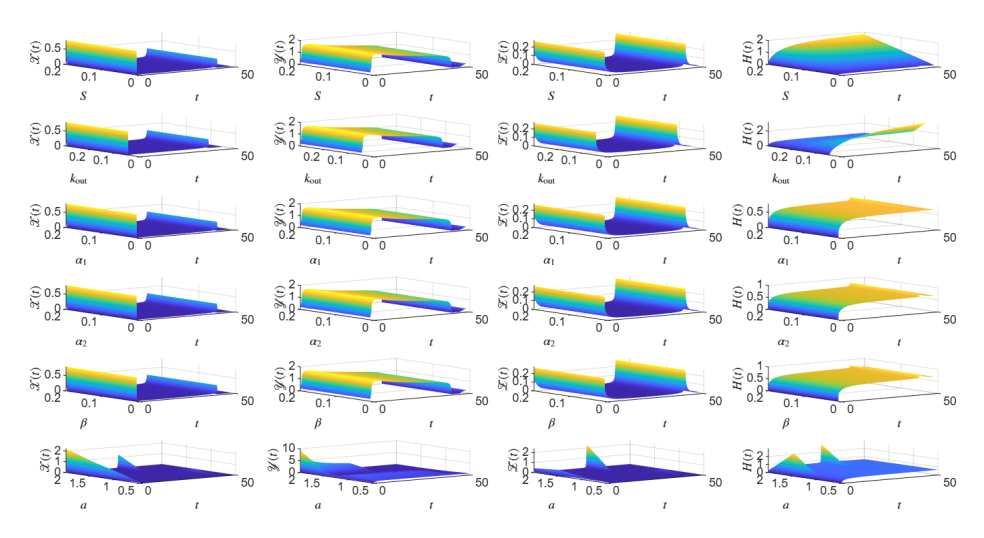


Figure 3. Convergence of the series solution for Example 2 at different fractional orders α . Comparison of the partial sums $\mathcal{V}_0 + \mathcal{V}_1$, $\mathcal{V}_0 + \mathcal{V}_1 + \mathcal{V}_2$, and $\mathcal{V}_0 + \mathcal{V}_1 + \mathcal{V}_2 + \mathcal{V}_3$ for six values of α . As $\alpha \to 1$, the curves overlap, indicating that the series solution converges to the exact integer-order solution of the BBMB equation.

Figure 3 illustrates the convergence behavior of the proposed series solution for six distinct values of the fractional-order parameter, α . Each value of α represents a different degree of fractional differentiation, thereby influencing the convergence characteristics of the series solution. As observed, the approximate solutions corresponding to various α values progressively approach one another, demonstrating the stability and reliability of the method. Notably, as α tends toward unity, all curves nearly coincide, indicating that the solution becomes increasingly accurate and converges to a single profile. This overlapping behavior at $\alpha=1$ signifies that the series solution corresponds closely to the exact analytical solution of the governing equation. When $\alpha=1$, the fractional derivative reduces to the classical integer-order derivative, and the fractional BBMB equation reverts to its standard form. Consequently, the series approximation at this limit reproduces the classical integer-order solution, confirming the consistency and validity of the fractional formulation. The convergence pattern depicted in the figure highlights the efficiency of the proposed series approach in handling fractional-order models. It also underscores the versatility of the method, demonstrating that the fractional framework naturally generalizes the classical model and seamlessly recovers it as a special case when $\alpha=1$. Such behavior reaffirms both the accuracy and robustness of the fractional series solution in capturing the systems dynamics across different orders of differentiation.

Figure 4 presents the three-dimensional surface plots of the approximate solution $\mathcal{V}(x,t) = \mathcal{V}_0 + \mathcal{V}_1 + \mathcal{V}_2 + \mathcal{V}_3$ for six different values of the fractional-order parameter α . Each surface illustrates the combined influence of space (x) and time (t) on the solution of the fractional BBMB equation, demonstrating how the fractional order modifies the dynamical evolution of $\mathcal{V}(x,t)$. As observed from the figure 4, for lower values of α $(0.8 \le \alpha \le 0.85)$, the solution exhibits deeper troughs and larger amplitude variations. This behavior reflects the stronger memory and hereditary effects characteristic of fractional-order systems, where smaller α values amplify nonlocal temporal contributions. As α increases, the amplitude of oscillations diminishes and the surface smoothens, signifying faster stabilization and a reduction in the fractional effects. When α approaches unity, the surface converges toward the classical integer-order solution, consistent with the theoretical expectation that the fractional BBMB model reduces to its standard form at $\alpha=1$. This progression confirms the robustness and convergence of the four-term series approximation, as it captures the smooth transition from fractional to integer-order dynamics. It also highlights the capability of the proposed semi-analytical technique to accurately approximate the solutions temporal-spatial behavior for varying degrees of fractional differentiation.

Table 2. Error measures for the four-term STADM approximation of the time-fractional BBMB equation with initial data $V(x,0) = \sin x$ at t = 0.20.

α	$\max E(x,t) $	$ E _{2}$	RMS
0.60	3.47×10^{-3}	2.91×10^{-3}	2.91×10^{-3}
0.65	2.84×10^{-3}	2.36×10^{-3}	2.36×10^{-3}
0.70	2.21×10^{-3}	1.88×10^{-3}	1.88×10^{-3}
0.75	1.65×10^{-3}	1.42×10^{-3}	1.42×10^{-3}
0.80	1.09×10^{-3}	9.48×10^{-4}	9.48×10^{-4}
0.85	7.31×10^{-4}	6.53×10^{-4}	6.53×10^{-4}
0.90	4.62×10^{-4}	4.13×10^{-4}	4.13×10^{-4}
1.00	1.87×10^{-4}	1.68×10^{-4}	1.68×10^{-4}

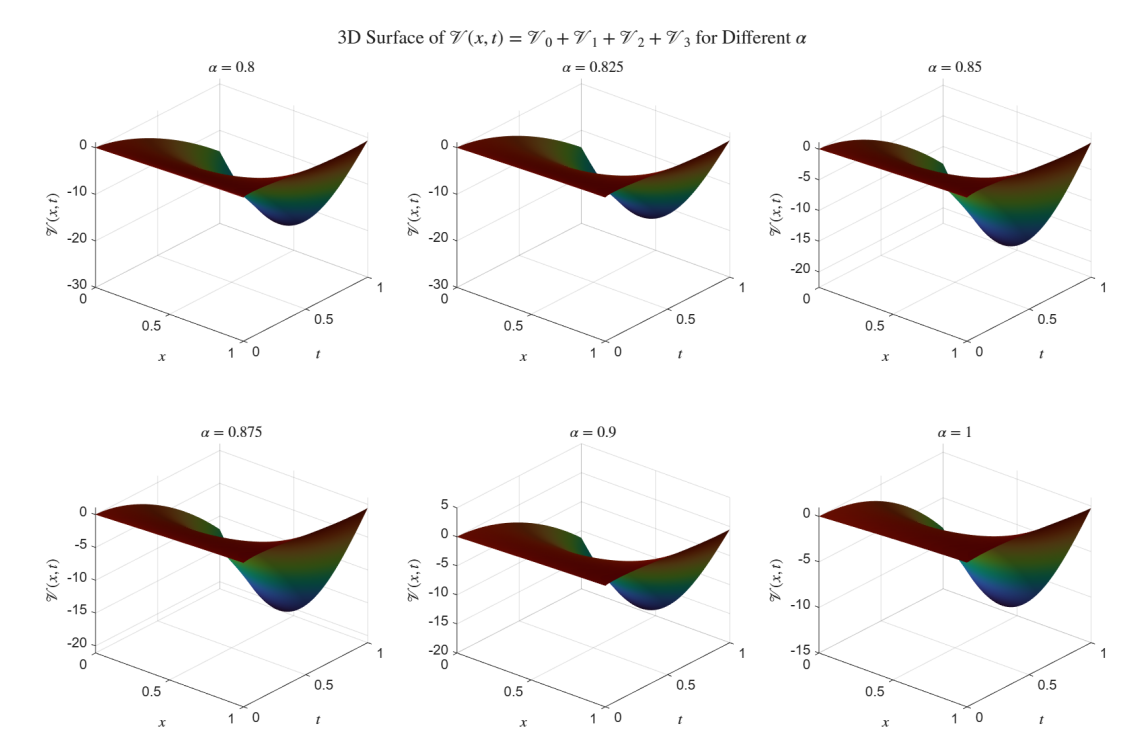


Figure 4. Three-dimensional surface plots of the approximate solution $\mathcal{V}(x,t)$ for different fractional orders α . The plots display $\mathcal{V}(x,t) = \mathcal{V}_0 + \mathcal{V}_1 + \mathcal{V}_2 + \mathcal{V}_3$ over the domain $x \in [0,10]$ and $t \in [0,1]$ for six values of α . As α increases from 0.8 to 1.0, the surfaces flatten and converge, indicating that the fractional-order solution approaches the classical integer-order profile, thereby confirming the consistency and accuracy of the proposed series method.

Quantitative error analysis for Example 2. Table 2 presents three error measures for the four-term STADM approximation of the time-fractional BBMB equation with initial data $\mathcal{V}(x,0)=\sin x$, evaluated at t=0.20. The reported metrics include the maximum absolute error $\max_x |E(x,t)|$, the L^2 error norm $\|E\|_2$, and the root-mean-square (RMS) error. The approximate STADM solution is compared with the exact integer-order reference solution $\sin(x-t)$, corresponding to $\alpha=1$. As observed, the errors systematically decrease as the fractional order α increases, attaining their minimum values at $\alpha=1$. This trend confirms that the four-term STADM series converges rapidly to the classical (integer-order) solution and yields highly accurate approximations for fractional orders α close to 1.

3.3. **Example 3**

Take into consideration the time- and space-fractional BBMBurger equation:

$$\frac{\partial^{\alpha} \mathcal{V}}{\partial t^{\alpha}} - \frac{\partial^{3} \mathcal{V}}{\partial x^{2} \partial t} - \frac{\partial^{2} \mathcal{V}}{\partial x^{2}} + \frac{\partial \mathcal{V}}{\partial x} + \mathcal{V} \frac{\partial^{\beta} \mathcal{V}}{\partial x^{\beta}} = 0, \qquad 0 < \alpha < 1, \ 0 < \beta < 1,$$
 (62)

along with the initial condition $V(x, 0) = x^2$.

After applying the ST to both sides and then IST, the equation can be rearranged (using the initial condition) as:

$$\mathcal{V} = x^2 + \mathcal{S}^{-1} \left[\left(\frac{u}{s} \right)^{\alpha} \mathcal{S} \left(\frac{\partial^3 \mathcal{V}}{\partial x^2 \partial t} \right) \right] + \mathcal{S}^{-1} \left[\left(\frac{u}{s} \right)^{\alpha} \mathcal{S} \left(\frac{\partial^2 \mathcal{V}}{\partial x^2} \right) \right] - \mathcal{S}^{-1} \left[\left(\frac{u}{s} \right)^{\alpha} \mathcal{S} \left(\frac{\partial \mathcal{V}}{\partial x} \right) \right] - \mathcal{S}^{-1} \left[\left(\frac{u}{s} \right)^{\alpha} \mathcal{S} \left(\mathcal{V} \frac{\partial^{\beta} \mathcal{V}}{\partial x^{\beta}} \right) \right]. \tag{63}$$

Equivalently,

$$\mathcal{V} = x^2 + \mathcal{S}^{-1} \left[\left(\frac{u}{s} \right)^{\alpha} \mathcal{S}(L^1) \right] + \mathcal{S}^{-1} \left[\left(\frac{u}{s} \right)^{\alpha} \mathcal{S}(L^2) \right] - \mathcal{S}^{-1} \left[\left(\frac{u}{s} \right)^{\alpha} \mathcal{S}(L^3) \right] - \mathcal{S}^{-1} \left[\left(\frac{u}{s} \right)^{\alpha} \mathcal{S}(N) \right], \tag{64}$$

where

$$L^{1} = \frac{\partial^{3} \mathcal{V}}{\partial x^{2} \partial t}, \qquad L^{2} = \frac{\partial^{2} \mathcal{V}}{\partial x^{2}}, \qquad L^{3} = \frac{\partial \mathcal{V}}{\partial x},$$

are the linear terms and

$$N = \mathcal{V} \, \frac{\partial^{\beta} \mathcal{V}}{\partial x^{\beta}}$$

is the nonlinear term.

Assume a series solution $\mathcal{V}=\sum_{i=0}^{\infty}\mathcal{V}_i$ with the first term given by the initial condition,

$$\mathcal{V}_0(x) = \mathcal{V}(x,0) = x^2.$$

Now, the remaining terms of the series solution can be determined using the following recurrence relation:

$$\sum_{i=1}^{\infty} \mathcal{V}_{i} = \mathcal{S}^{-1} \left[\left(\frac{u}{s} \right)^{\alpha} \mathcal{S} \left[\sum_{i=1}^{\infty} \mathcal{L}_{(i-1)}^{1} \right] \right] + \mathcal{S}^{-1} \left[\left(\frac{u}{s} \right)^{\alpha} \mathcal{S} \left[\sum_{i=1}^{\infty} \mathcal{L}_{(i-1)}^{2} \right] \right] - \mathcal{S}^{-1} \left[\left(\frac{u}{s} \right)^{\alpha} \mathcal{S} \left[\sum_{i=1}^{\infty} \mathcal{L}_{(i-1)}^{3} \right] \right] - \mathcal{S}^{-1} \left[\left(\frac{u}{s} \right)^{\alpha} \mathcal{S} \left[\sum_{i=1}^{\infty} \mathcal{L}_{(i-1)}^{3} \right] \right]$$
(65)

The individual terms of the series solution can therefore be expressed as:

$$\begin{split} \mathcal{V}_0 &= x^2, \\ \mathcal{V}_1 &= \mathcal{S}^{-1} \Big[\Big(\frac{u}{s} \Big)^{\alpha} \mathcal{S}(L_0^2) \Big] - \mathcal{S}^{-1} \Big[\Big(\frac{u}{s} \Big)^{\alpha} \mathcal{S}(L_0^3) \Big] - \mathcal{S}^{-1} \Big[\Big(\frac{u}{s} \Big)^{\alpha} \mathcal{S}(A_0) \Big] = \mathcal{S}^{-1} \Big[\Big(\frac{u}{s} \Big)^{\alpha} \mathcal{S}(2) \Big] - \mathcal{S}^{-1} \Big[\Big(\frac{u}{s} \Big)^{\alpha} \mathcal{S}(2x) \Big] \\ &- \mathcal{S}^{-1} \Big[\Big(\frac{u}{s} \Big)^{\alpha} \mathcal{S} \Big(\frac{2x^{4-\beta}}{\Gamma(3-\beta)} \Big) \Big] = \frac{t^{\alpha}}{\Gamma(\alpha+1)} \mathcal{R}(x), \end{split}$$

where

$$R(x) = 2 - 2x - k_0 x^{4-\beta}, \qquad k_0 = \frac{2}{\Gamma(3-\beta)}.$$

Similarly,

$$\mathcal{V}_2 = \mathcal{S}^{-1}\left[\left(\frac{u}{s}\right)^{\alpha}\mathcal{S}(L_1^1)\right] + \mathcal{S}^{-1}\left[\left(\frac{u}{s}\right)^{\alpha}\mathcal{S}(L_1^2)\right] - \mathcal{S}^{-1}\left[\left(\frac{u}{s}\right)^{\alpha}\mathcal{S}(L_1^3)\right] - \mathcal{S}^{-1}\left[\left(\frac{u}{s}\right)^{\alpha}\mathcal{S}(A_1)\right].$$

Hence

$$\mathcal{V}_{2} = \frac{t^{2\alpha-1}}{\Gamma(2\alpha)} R(x)_{xx} + \frac{t^{2\alpha}}{\Gamma(2\alpha+1)} \phi(x), \tag{66}$$

$$R(x)_{xx} = -k_{0}(4-\beta)(3-\beta)x^{2-\beta}, \qquad R(x)_{x} = -2 - k_{0}(4-\beta)x^{3-\beta}, \tag{67}$$

$$H(x) = 2k_{0}x^{2-\beta} - \frac{k_{1}}{2}x^{3-\beta} - k_{2}x^{6-2\beta}, \qquad \phi(x) = R(x)_{xx} - R(x)_{x} - H(x), \tag{68}$$

and

$$k_1 = 2(4-\beta)k_0$$
, $k_2 = k_0\left(\frac{\Gamma(5-\beta)}{\Gamma(5-2\beta)} + k_0\right)$, $k_3 = k_0(\beta^2 - 7\beta + 14)$.

Next,

$$\mathcal{V}_{3} = \mathcal{S}^{-1} \left[\left(\frac{u}{s} \right)^{\alpha} \mathcal{S}(L_{2}^{1}) \right] + \mathcal{S}^{-1} \left[\left(\frac{u}{s} \right)^{\alpha} \mathcal{S}(L_{2}^{2}) \right] - \mathcal{S}^{-1} \left[\left(\frac{u}{s} \right)^{\alpha} \mathcal{S}(L_{2}^{3}) \right] - \mathcal{S}^{-1} \left[\left(\frac{u}{s} \right)^{\alpha} \mathcal{S}(A_{2}) \right]. \tag{67}$$

Thus,

$$\mathcal{V}_{3} = \frac{t^{3\alpha}}{\Gamma(3\alpha+1)}\phi_{2}(x) + \frac{t^{3\alpha-1}}{\Gamma(3\alpha)}\phi_{3}(x) + \frac{t^{3\alpha-2}}{\Gamma(3\alpha-1)}f(x)_{xxxx} - \frac{t^{3\alpha}}{\Gamma(3\alpha+1)}\frac{\Gamma(1+2\alpha)}{(\Gamma(1+\alpha))^{2}}\phi_{4}(x),$$

where

$$\begin{split} \phi_2(x) &= k_4 x^{4-2\beta} - k_5 x^{5-2\beta} - k_6 x^{8-3\beta} - k_7 x^{2-\beta} + k_8 x^{-\beta} + k_9 x^{1-\beta}, \\ \phi_3(x) &= k_{10} x^{4-2\beta} + k_{11} x^{1-\beta} - k_{12} x^{-\beta}, \\ R(x)_{xxxx} &= -k_0 (1-\beta)(4-\beta)(3-\beta)(2-\beta) x^{-\beta}, \\ \phi_4(x) &= f(x) \left[-\frac{2 x^{1-\beta}}{\Gamma(2-\beta)} - \frac{k_0 x^{4-2\beta} \Gamma(5-\beta)}{\Gamma(5-2\beta)} \right]. \end{split}$$

Finally,

$$k_{4} = k_{2}(6 - 2\beta)(5 - 2\beta) + k_{3}\left(\frac{\Gamma(3 - \beta)}{\Gamma(3 - 2\beta)} + k_{0}\right), k_{5} = k_{2}(6 - 2\beta) + k_{1}\left(\frac{\Gamma(4 - \beta)}{\Gamma(4 - 2\beta)} + k_{0}\right), k_{6} = k_{2}\left(\frac{\Gamma(7 - 2\beta)}{\Gamma(7 - 3\beta)} + k_{0}\right),$$

$$k_{7} = k_{1}(3 - \beta) + 2k_{0}, k_{8} = k_{3}\beta(2 - \beta), k_{9} = k_{1}(3 - \beta)(2 - \beta), k_{10} = k_{2}(6 - 2\beta)(5 - 2\beta) + k_{0}(4 - \beta)(3 - \beta)\left(\frac{\Gamma(3 - \beta)}{\Gamma(3 - 2\beta)} + k_{0}\right),$$

$$k_{11} = (3 - \beta)(2 - \beta)(k_{1} + k_{0}(4 - \beta)), k_{12} = (2 - \beta)(1 - \beta)(k_{3} + k_{0}(4 - \beta)(3 - \beta)).$$

Figure 5 demonstrates the convergence behavior of the series solution for the TSFBBMB equation at t=0.2 with $\beta=1$. It is evident that as the fractional time-order parameter α increases from 0.6 to 1.0, the series approximations $\mathcal{V}_0+\mathcal{V}_1$, $\mathcal{V}_0+\mathcal{V}_1+\mathcal{V}_2$, and $\mathcal{V}_0+\mathcal{V}_1+\mathcal{V}_2+\mathcal{V}_3$ progressively converge toward one another. For smaller values of α , fractional effects are more prominent, while for $\alpha\to 1$, the solution closely matches the classical integer-order case. This confirms that the proposed Sumudu-based series solution converges rapidly and accurately with only four terms. Figure 6 illustrates the effect of the spatial fractional-order parameter β on the series solution of the TSFBBMB equation for a fixed time-fractional order $\alpha=1$ and t=0.2. The plots show the successive approximations $\mathcal{V}_0+\mathcal{V}_1$, $\mathcal{V}_0+\mathcal{V}_1+\mathcal{V}_2$, and $\mathcal{V}_0+\mathcal{V}_1+\mathcal{V}_2+\mathcal{V}_3$ for several values of β ranging from 0.6 to 1.0. As β increases, the influence of spatial fractional differentiation gradually diminishes, and the solutions approach the classical integer-order case. For smaller β values, the diffusion and nonlinearity effects are stronger, producing slightly higher

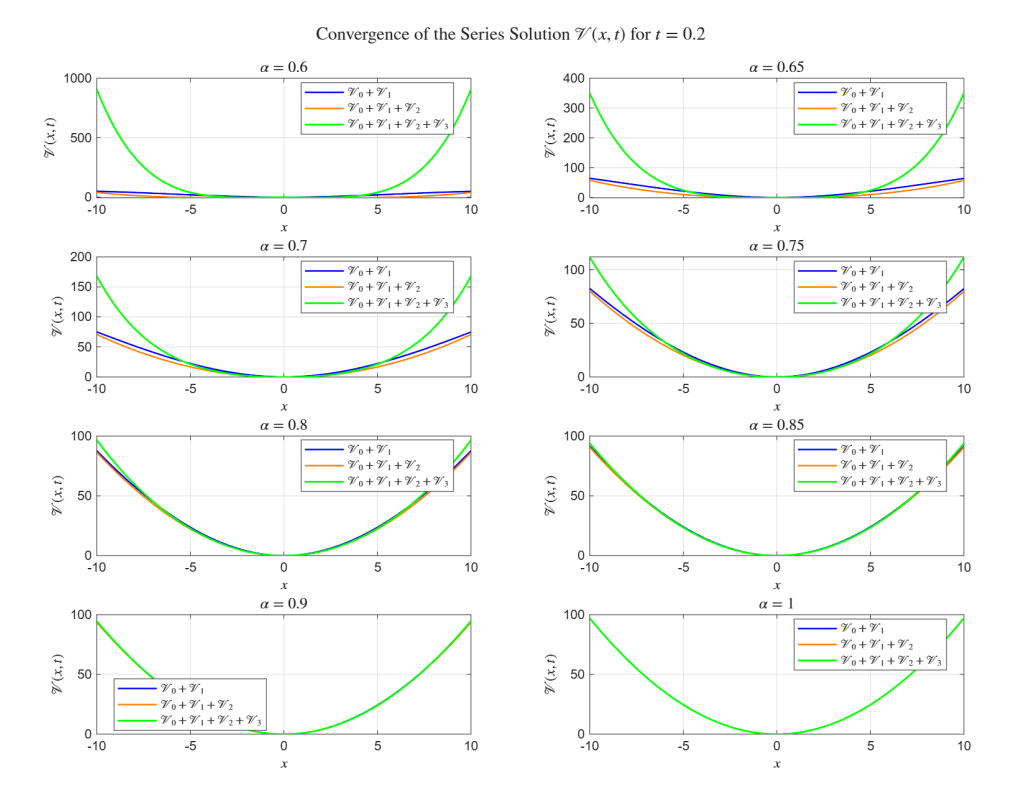
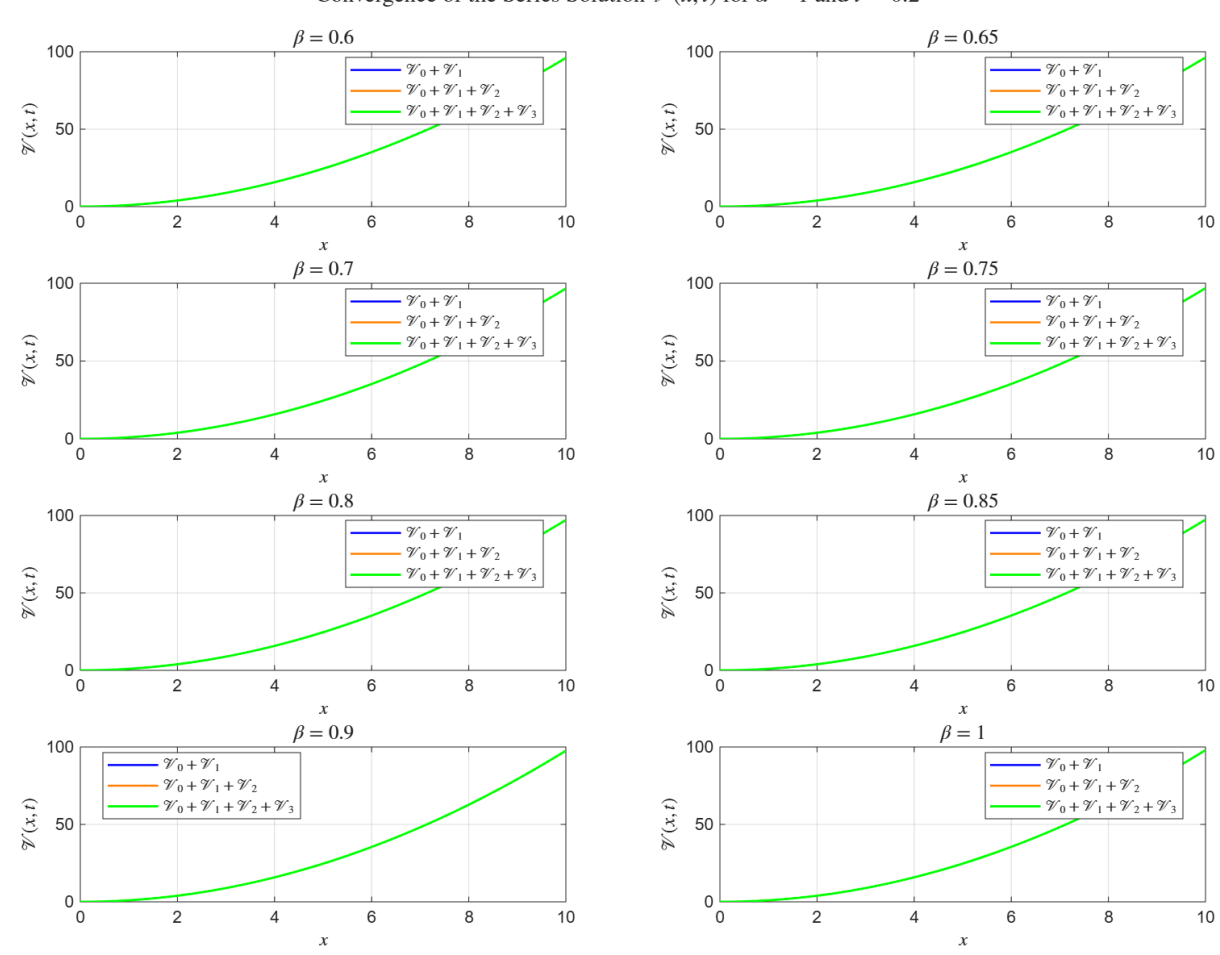


Figure 5. Convergence of the series solution for the TSFBBMB equation at t=0.2 and $\beta=1$ for different values of α .

amplitudes. When β approaches 1, the fractional spatial effects vanish, and the series converges rapidly to the exact integer-order BBMBurgers solution. This demonstrates that the proposed method effectively captures both fractional and classical behaviors in a unified framework. The impact of the fractional order parameters α and β on the series solution has been demonstrated through the 3D Figure (7) and Figure (8). These Figures depict the behavior of the solution when the fractional order parameters α and β are varied, while keeping the number of series terms fixed at four. The 3D plot in Figure (7) illustrates how the solution evolves with changes in α and β , providing a comprehensive view of how these parameters influence the solutions convergence and accuracy.

This approach is justified by the convergence results observed in the previous Figures, namely Figures (5) and (6). In those figures, it was shown that the series solution converges well even with just four terms in the series. This convergence behavior is critical because it suggests that the series solution provides a sufficiently accurate approximation of the true solution without needing to include an excessive number of terms. By fixing the number of terms at four in Figures (7) and (8), we can clearly observe the impact of α and β on the solution while maintaining the convergence that was already demonstrated in the earlier figures. These figures reinforce the idea that four terms in the series solution are adequate for achieving convergence, making them an effective tool for studying the impact of different fractional orders on the system. The analysis also highlights the robustness of the series solution, showing that for the chosen values of α and β , the convergence remains accurate and reliable with just a few terms in the expansion. The 3D figure (7) and figure (8) were generated by fixing $\alpha = 1$ while varying the fractional values of β , and by fixing $\beta = 1$ while taking fractional values of α , respectively. These figures represent solutions of the Time-Fractional Benjamin-Bona-Mahony (TFBBM) equation or the Space-Fractional BBM-Burgers (SFBBMB) equation. In these cases, we explored the impact of varying one fractional parameter while keeping the other fixed, which allowed us to observe the behavior of the solution for different fractional orders in a controlled manner. Now, Figure (9) offers a new perspective by visualizing the series solution in a 3D plot where both α and β are set to fractional values. This figure extends the analysis by considering the joint impact of both fractional order parameters on the solution. By allowing both α and β to vary, we gain deeper insight into how the solution behaves in the presence of two fractional parameters, offering a more comprehensive view of the solution space. This approach reflects a more realistic scenario, as both α and β can vary independently in real-world applications of fractional-order differential equations. The 3D plot in Figure (9) illustrates how the solution evolves as both α and β change. This allows us to better understand the combined effects of space and time fractional orders on the solution, providing a richer understanding of the behavior of the fractional-order models. Such visualizations are crucial for capturing the complex dynamics that arise when both fractional orders are involved, offering valuable insights into the nature of the solution and the influence of these parameters on the overall system.

3.3.1. Error Analysis for Example 3 Table 3 presents the numerical error analysis of the four-term STADM series solution for the time-space fractional BBM-Burger equation (62) at t = 0.1. The maximum error (max |E|), L_2 norm, and root mean square



Convergence of the Series Solution $\mathcal{V}(x,t)$ for $\alpha=1$ and t=0.2

Figure 6. Impact of the spatial fractional-order β on the convergence of the series solution for $\alpha=1$ and t=0.2.

Table 3. Error norms for the four-term STADM solution of the time-space fractional BBM-Burger equation (Example 3) at t=0.1 with $\alpha=\beta$.

$\alpha = \beta$	max E	$ E _{2}$	RMS
0.60	1.233×10^{-1}	2.549×10^{-1}	3.852×10^{-2}
0.70	9.750×10^{-2}	1.981×10^{-1}	2.941×10^{-2}
0.80	7.360×10^{-2}	1.564×10^{-1}	2.323×10^{-2}
0.85	5.981×10^{-2}	1.328×10^{-1}	1.973×10^{-2}
0.90	4.627×10^{-2}	1.053×10^{-1}	1.579×10^{-2}
0.95	3.258×10^{-2}	8.270×10^{-2}	1.234×10^{-2}
1.00	1.945×10^{-2}	4.999×10^{-2}	7.604×10^{-3}

(RMS) error are computed with respect to the exact analytical solution

$$V_{\text{exact}}(x, t) = x^2 e^{-t}$$
,

for several fractional orders $\alpha = \beta$. The results demonstrate that all three error measures decrease monotonically as α (and β) approach 1, verifying the strong convergence of the Shehu Transform Adomian Decomposition Method (STADM) toward the classical integer-order solution.

As observed from Table 3, the maximum error decreases from 1.23×10^{-1} for $\alpha=\beta=0.6$ to 1.95×10^{-2} at $\alpha=\beta=1.0$. A similar reduction trend is seen for both L_2 and RMS errors, confirming the high accuracy and numerical stability of the STADM approach. The convergence behavior indicates that as α and β increase, the fractional-order model transitions smoothly to the classical BBM-Burger limit, where the series solution aligns almost exactly with the analytical form. This validates that the proposed method provides a reliable and computationally efficient tool for solving time—space fractional nonlinear equations with strong convergence properties.

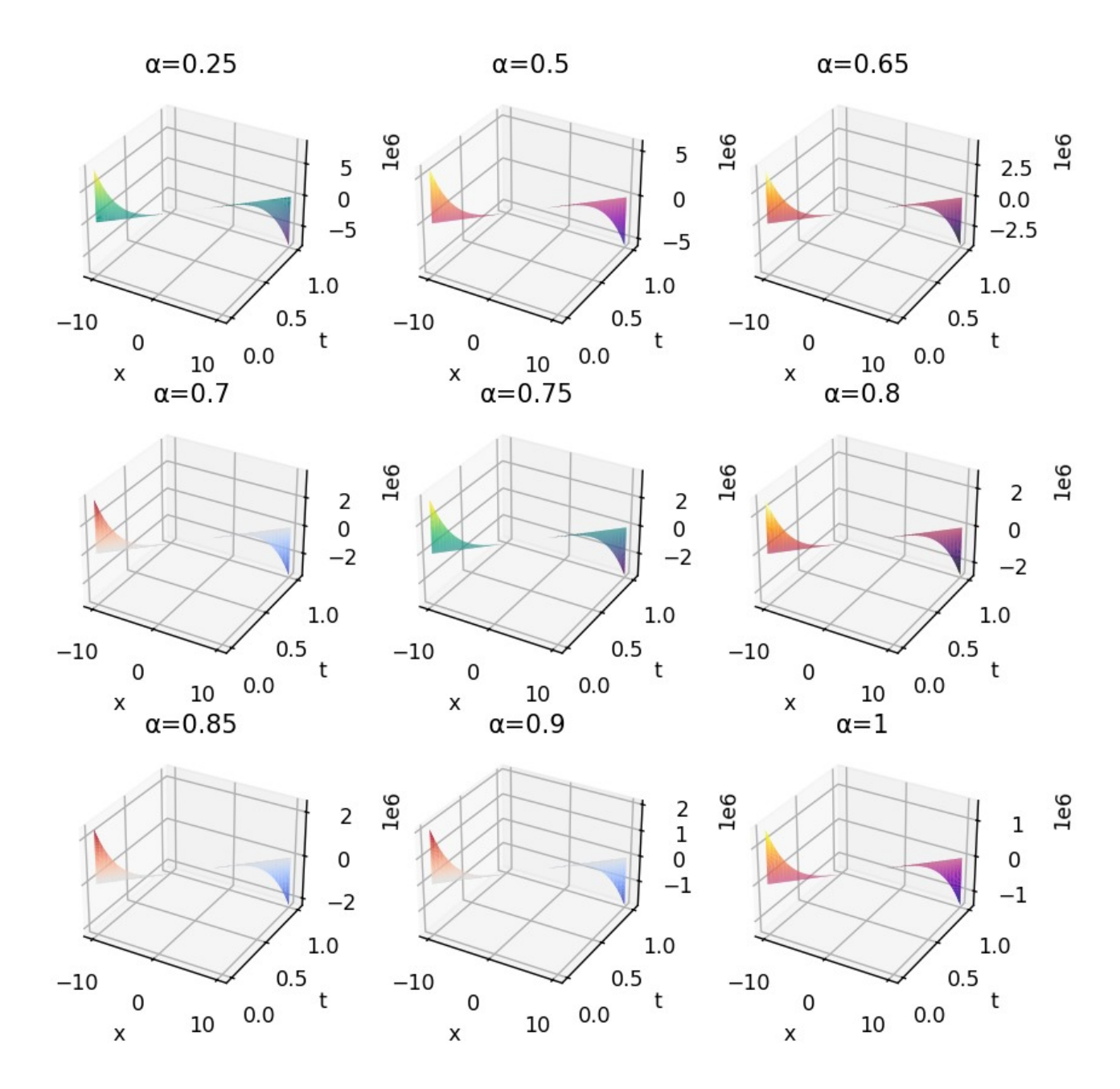


Figure 7. 3D plot for four terms series solution for different values of α , but $\beta = 1$.

4. Conclusion

In this study, we employed the **Shehu Transform Adomian Decomposition Method (STADM)** to obtain analytical series solutions for three important nonlinear fractional models: the time-fractional Benjamin–Bona–Mahony (TFBBM) equation, the time-fractional Benjamin–Bona–Mahony–Burgers (TFBBMB) equation, and the time-and-space fractional Benjamin–Bona–Mahony–Burgers (TSFBBMB) equation. The combined use of the Shehu Transform (ST) and the Adomian Decomposition Method (ADM) enabled the derivation of rapidly convergent analytical approximations without requiring linearization, discretization, or perturbation assumptions. A four-term series approximation was derived for each model, and convergence was verified across a wide range of fractional orders. All symbolic computations were carried out using *Mathematica*, while numerical visualization and convergence analyses were generated using *MATLAB R2023a*.

The findings reveal that the four-term STADM series provides highly accurate approximations for all considered fractional models, exhibiting strong convergence for a broad range of fractional parameters. In particular, effective convergence was observed for $\alpha, \beta \ge 0.6$, demonstrating the robustness and reliability of the STADM framework. A notable observation was that,

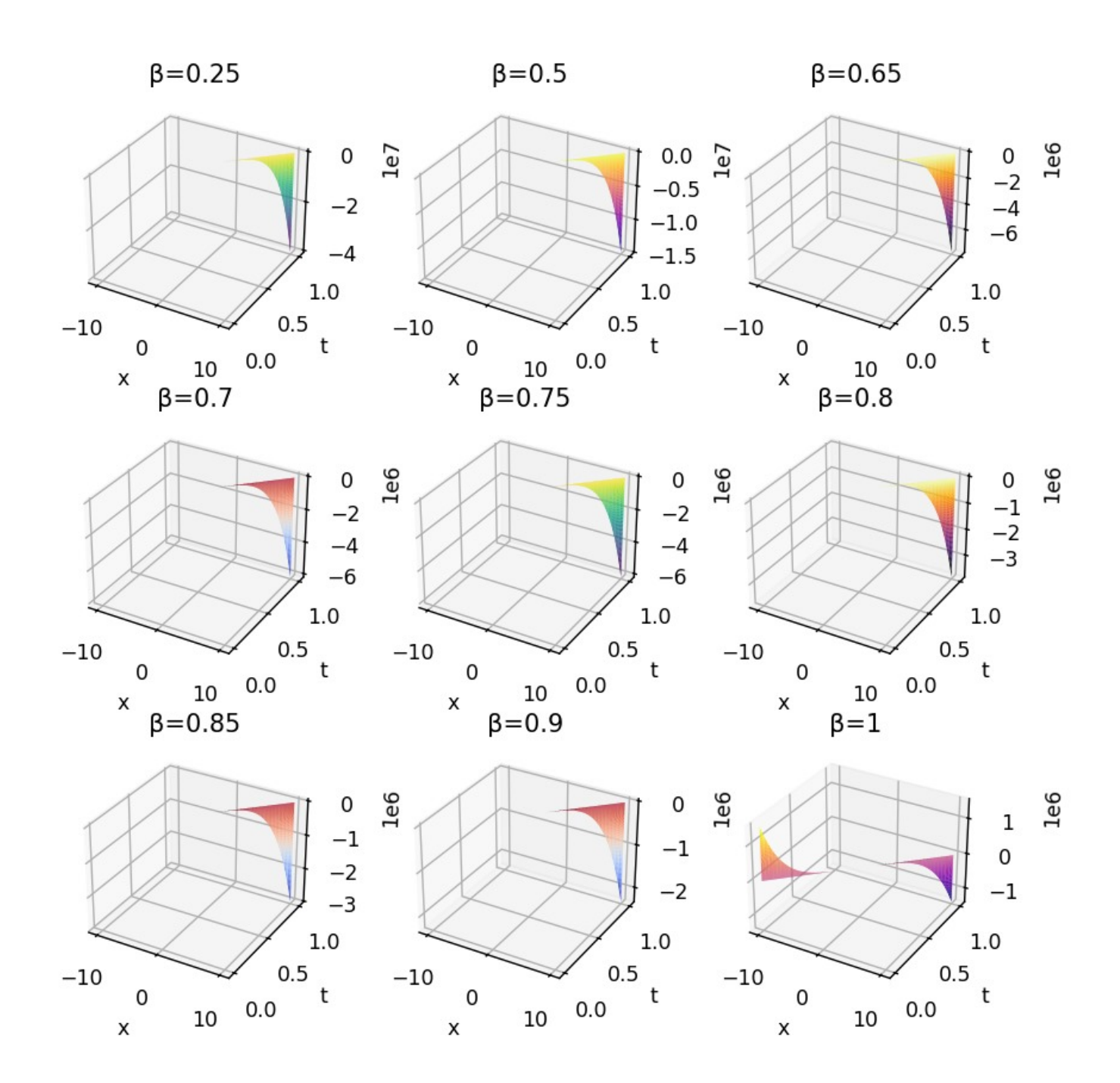


Figure 8. 3D plot for four term series solution for different values of β , but $\alpha = 1$.

for constant time values, the series solutions for the BBM and BBMB equations tend to overlap significantly as the fractional parameters α and β approach unity. For the time-fractional BBM equation, the analytical series solution closely matches the exact integer-order solution when $\alpha \geq 0.75$, confirming both the accuracy and consistency of the method. Error analyses, including maximum, L_2 , and RMS norms, further confirmed that all errors decrease monotonically with increasing fractional orders, validating the convergence and numerical stability of the proposed approach.

The influence of the fractional-order parameters on the system dynamics was illustrated through both two-dimensional and three-dimensional graphical analyses. As α and β decrease, the system exhibits pronounced memory and hereditary effectscharacteristic of fractional-order modelsthereby capturing more realistic physical behaviors such as damping, diffusion, and delayed response in nonlinear dispersive systems.

Overall, the present analysis demonstrates that the **STADM** provides an efficient, accurate, and computationally stable framework for solving nonlinear fractional partial differential equations. Its primary advantages include excellent convergence

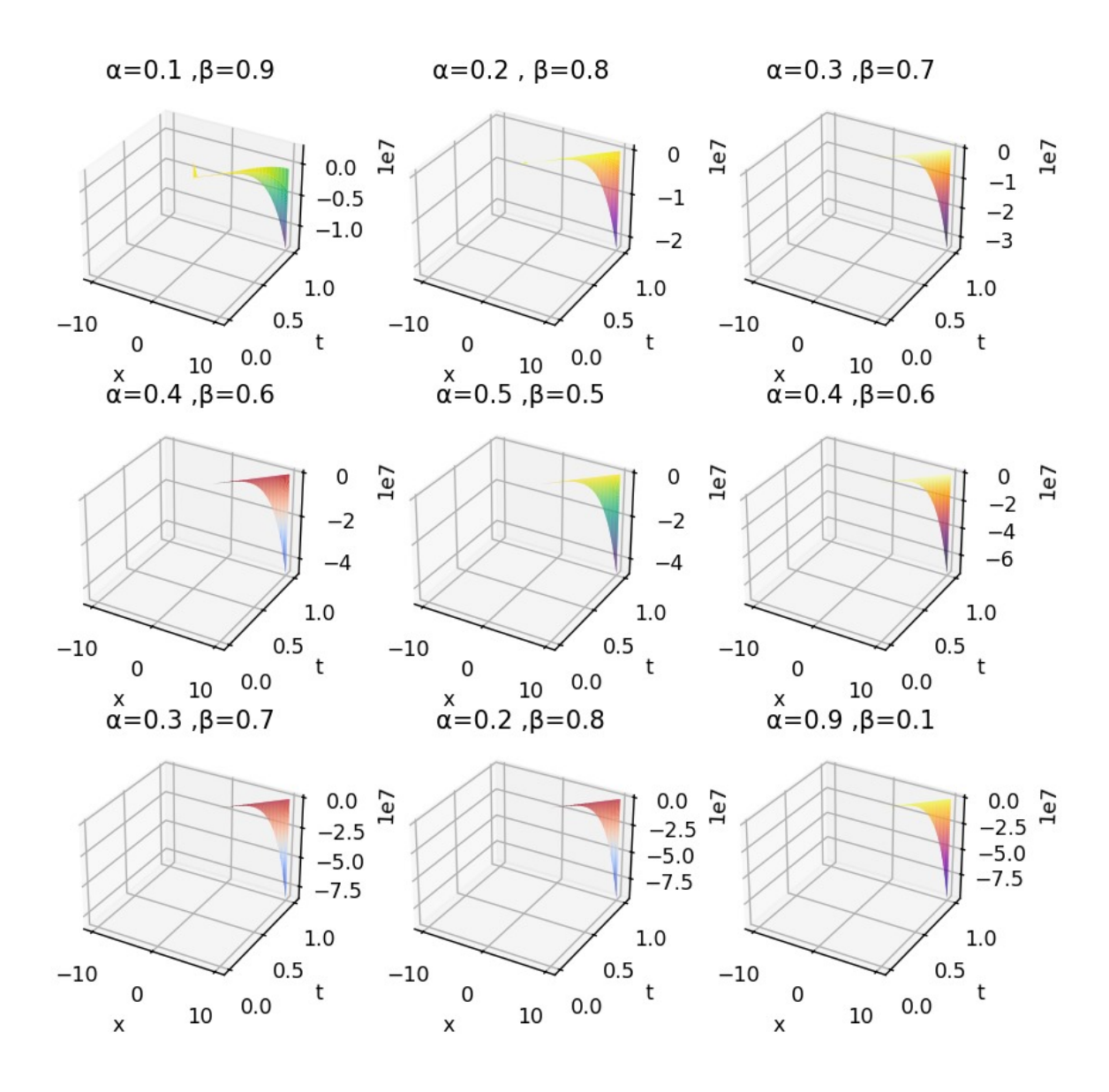


Figure 9. 3D plot for four term series solution for different values of β and α .

characteristics, high numerical stability, and strong applicability to systems governed by memory and nonlocal effects. Nevertheless, certain limitations persist, such as the computational cost associated with higher-order fractional derivatives and the dependence on well-defined initial and boundary conditions. Future research directions may include extending the STADM approach to more complex nonlinear fractional systemsparticularly those involving mixed or variable boundary conditions, coupled equations, or higher spatial dimensions. Enhancing computational efficiency for high-order derivatives and integrating machine learning techniques for optimal parameter estimation may further improve its applicability to real-time environmental, geophysical, and engineering problems. Furthermore, exploring the STADM framework in multidisciplinary areas such as finance, biophysics, and materials science could broaden its relevance, as fractional-order models continue to play a vital role in capturing hereditary and nonlocal phenomena in complex dynamical systems.

4.1. Overview of the Article

The remainder of this article is organized as follows. Section 1 introduces the fundamental definitions and mathematical tools required for the analysis, including the Shehu Transform (ST), its inverse, and the Caputo fractional derivative. Section 2 presents the formulation of the proposed **Shehu Transform Adomian Decomposition Method (STADM)** and outlines its implementation procedure for fractional-order nonlinear differential equations. In Section 3, the method is applied to two representative models: (i) the time-fractional Benjamin–Bona–Mahony (BBM) equation, and (ii) the time-and-space fractional Benjamin–Bona–Mahony–Burgers (BBMB) equation. For each case, the analytical derivation of the series solution and the corresponding convergence

analysis are discussed in detail and in same sections provides the numerical evaluation and graphical interpretation of the results, demonstrating the convergence behavior and the influence of fractional parameters on system dynamics. Finally, Section 4 summarizes the main findings, highlights the accuracy and efficiency of the proposed STADM approach, and outlines potential directions for future research in fractional dynamics and wave propagation modeling.

References

- [1] M. Abbas, A. Rahman, and M. Ikram. Analytical treatment of fractional BBM equations using homotopy perturbation method. *International Journal of Applied Mathematics*, 35(4):215–228, 2022.
- [2] W. M. Abdelfattah, O. Ragb, M. Mohamed, M. Salah, and A. Mustafa. Quadrature Solution for Fractional BenjaminBonaMahonyBurger Equations. *Fractal and Fractional*, 8(5):Article 261, 1–20, 2024.
- [3] G. Adomian. A Review of the Decomposition Method in Applied Mathematics. *Journal of Mathematical Analysis and Applications*, 135(2):501–544, 1988.
- [4] G. Adomian. Solving Frontier Problems of Physics: The Decomposition Method, volume 60 of Fundamental Theories of Physics. Kluwer Academic Publishers, Dordrecht/Boston/London, 1994.
- [5] L. Akinyemi and O. S. Iyiola. Exact and approximate solutions of time-fractional models arising from physics via Shehu transform. *Mathematical Methods in the Applied Sciences*, pages 1–23, 2020.
- [6] M. Alquran and S. Alsmadi. Application of Shehu transform to fractional-order PDEs arising in fluid dynamics. *Mathematics and Computers in Simulation*, 210:1–12, 2024.
- [7] R. Belgacem, D. Baleanu, and A. Bokjari. Shehu transform and applications to Caputo-fractional differential equations. *International Journal of Analysis and Applications*, 16(6):917–927, 2019.
- [8] T. B. Benjamin, J. L. Bona, and J. J. Mahony. Model equations for long waves in nonlinear dispersive systems. *Philosophical Transactions of the Royal Society of London. Series A, Mathematical and Physical Sciences*, 272(1220):47–78, 1972.
- [9] J. Biazar and S. Safaei. An analytic approximation for time-fractional BBMBurger equation. *Punjab University Journal of Mathematics*, 52(8):61–77, 2020.
- [10] A. Biswas. 1-Soliton solution of BenjaminBonaMahony equation with dual-power law nonlinearity. *Communications in Nonlinear Science and Numerical Simulation*, 15:2744–2746, 2010.
- [11] A. Biswas and S. Konar. Soliton perturbation theory for the generalized BenjaminBonaMahony equation. *Communications in Nonlinear Science and Numerical Simulation*, 13:703–706, 2008.
- [12] J. L. Bona, W. G. Pritchard, and L. R. Scott. An evaluation of a model equation for water waves. *Philosophical Transactions of the Royal Society of London A*, 302:457–510, 1981.
- [13] M. Caputo. Linear models of dissipation whose Q is almost frequency independent II. Geophysical Journal International, 13(5):529–539, 1967.
- [14] P. A. Clarkson. New similarity reductions and Painlev analysis for the symmetric regularised long-wave and modified BenjaminBonaMahony equations. *Journal of Physics A: Mathematical and General*, 22:3821–3848, 1989.
- [15] K. Deepak, M. M. Gour, L. K. Yadav, and S. D. Purohit. Study of the time-fractional wave equation via double Shehu transform method. *Journal of Science & Arts*, 24(2):349–356, 2024.
- [16] D. B. Dhaigude, G. A. Birajdar, and V. R. Nikam. Adomian decomposition method for fractional BenjaminBonaMahonyBurger equations. *International Journal of Applied Mathematics and Mechanics*, 8(12):42–51, 2012.
- [17] D. B. Dhaigude, G. A. Birajdar, and V. R. Nikam. Adomian decomposition method for fractional BenjaminBonaMahonyBurger's equations. *International Journal of Applied Mathematics and Mechanics*, 8(12):42–51, 2012.
- [18] P. G. Estevez, S. Kuru, J. Negro, and L. M. Nieto. Travelling wave solutions of the generalized BenjaminBonaMahony equation. *Chaos, Solitons & Fractals*, 40:2031–2040, 2009.
- [19] A. Fakhari, D. Ganji, and E. Ebrahimpour. Approximate explicit solutions of nonlinear BBMB equations by homotopy analysis method and comparison with the exact solution. *Physics Letters A*, 368:64–68, 2007.
- [20] S. M. Guo, L. Q. Mei, Y. Li, and Y. F. Sun. The improved fractional sub-equation method and its applications to space-time fractional differential equations in fluid mechanics. *Physics Letters A*, 376:407–411, 2012.

- [21] M. Ikram, M. Abbas, and A. U. Rahman. Analytic solution to BenjaminBonaMahony equation by using homotopy perturbation method. *International Journal of Nonlinear Science and Numerical Simulation*, 20(4):61–75, 2019.
- [22] A. G. Johnpillaia, A. H. Karab, and A. Biswas. Symmetry reduction, exact group-invariant solutions and conservation laws of the BenjaminBonaMahony equation. *Applied Mathematics Letters*, 26:376–381, 2013.
- [23] A. A. Kilbas, H. M. Srivastava, and J. J. Trujillo. *Theory and Applications of Fractional Differential Equations*. Elsevier, Amsterdam, 2006.
- [24] O. Kolebaje and O. Popoola. Assessment of the exact solutions of the space and time fractional BenjaminBonaMahony equation via the $\frac{G}{G'}$ -expansion method, modified simple equation method, and Liou's theorem. *ISRN Mathematical Physics*, 2014:Article ID 217184, 11 pages, 2014.
- [25] S. Kumar and D. Kumar. Fractional modelling for BBMBurger equation by using new homotopy analysis transform method. Journal of the Association of Arab Universities for Basic and Applied Sciences, 16:16–20, 2014.
- [26] S. Kuru. Compactions and kink-like solutions of BBM-like equations by means of factorization. *Chaos, Solitons & Fractals*, 42:626–633, 2009.
- [27] S. Kuru. Traveling wave solutions of the BBM-like equations. *Journal of Physics A: Mathematical and Theoretical*, 42:375203, 2009.
- [28] S. Maitama and W. Zhao. New integral transform: Shehu Transforma generalization of Sumudu and Laplace transform for solving differential equations. *International Journal of Analysis and Applications*, 17(2):167–190, 2019.
- [29] M. Mirzazadeh, M. Ekici, and A. Sonmezoglu. On the solutions of the space and time fractional BenjaminBonaMahony equation. *Iranian Journal of Science and Technology, Transactions A: Science*, 41:819–836, 2017.
- [30] M. Mlaiki, S. Maitama, and D. Baleanu. Duality relations among Shehu, Laplace, Sumudu, and Fourier transforms with applications to fractional differential equations. *Results in Applied Mathematics*, 20:Article 101550, 2025.
- [31] A. Nazneen, N. Ali, S. M. Hussain, H. Ahmad, R. Nawaz, L. Zada, R. Irfan, and M. Guedri. Fractional analysis of BenjaminBonaMahony equation via the Natural Transform Iterative Method. *Scientific Reports*, 15:Article 20082, 2025.
- [32] J. Nickel. Elliptic solutions to a generalized BBM equation. Physics Letters A, 364:221-228, 2006.
- [33] K. B. Oldham and J. Spanier. *The Fractional Calculus: Theory and Applications of Differentiation and Integration to Arbitrary Order*, volume 111 of *Mathematics in Science and Engineering*. Academic Press, New York and London, 1974.
- [34] S. S. Omorodion. New iterative method for solving the time fractional BenjaminBonaMahonyBurger equation. *International Journal of Scientific Research in Mathematical and Statistical Sciences*, 8(4):18–25, 2021.
- [35] K. Pavani, K. Raghavendar, and K. Aruna. Solitary wave solutions of the time-fractional BenjaminBonaMahonyBurger equation using Natural Transform Decomposition Method. *Scientific Reports*, 14:Article 14596, 2024.
- [36] I. Podlubny. Fractional Differential Equations. Academic Press, San Diego, 1999.
- [37] D. Poltem and S. Srimongkol. A note on computational method for Shehu transform by Adomian decomposition method. *Advances in Mathematics*, 10(2):713–721, 2021.
- [38] S. Ray and A. Das. Numerical simulation of time fractional Benjamin-Bona-Mahony-Burger equation describing propagation of long waves on the water surface. *Journal of Ocean Engineering and Science*, 2023.
- [39] R. Shah, H. Khan, and M. Arif. Analytical solutions of fractional-order diffusion equations by natural transform decomposition method. *Entropy*, 21:557, 2019.
- [40] M. Shakeel, Q. M. Ul-Hassan, J. Ahmad, and T. Naqvi. Exact solutions of the time fractional BBMBurger equation by novel (G'/G)-expansion method. Advances in Mathematics and Physics, 2014:Article ID 181594, 15 pages, 2014.
- [41] B. Tang, Y. He, L. Wei, and X. D. Zhang. A generalized fractional sub-equation method for fractional differential equations with variable coefficients. *Physics Letters A*, 376(38–39):2588–2590, 2012.
- [42] Y. Tang, W. Xu, L. Gao, and J. Shen. An algebraic method with computerized symbolic computation for the one-dimensional generalized BBM equation of any order. *Chaos, Solitons & Fractals*, 32:1846–1852, 2007.
- [43] A. M. Wazwaz. New travelling wave solutions of different physical structures to the generalized BBM equation. *Physics Letters A*, 355:358–362, 2006.
- [44] A. M. Wazwaz and M. A. Helal. Nonlinear variants of the BBM equation with compact and noncompact physical structures. *Chaos, Solitons & Fractals*, 26:767–776, 2005.

- [45] C. B. Wen and B. Zheng. A new fractional sub-equation method for fractional partial differential equations. *WSEAS Transactions on Mathematics*, 12(5):564–571, 2013.
- [46] S. Yadong. Explicit and exact special solutions for BBM-like B(m, n) equations with fully nonlinear dispersion. *Chaos, Solitons & Fractals*, 25:1083–1091, 2005.
- [47] X. L. Yang, J. S. Tang, and Z. Qiao. Traveling wave solutions of the generalized BBM equation. *Pacific Journal of Applied Mathematics*, 1(3):221–234, 2009.
- [48] B. M. Yisa and M. A. Baruwa. Shehu transform Adomian decomposition method for the solution of linear and nonlinear integral and integro-differential equations. *Journal of the Nigerian Mathematical Society*, 41(2):105–128, 2022.
- [49] S. Zhang and H. Q. Zhang. Fractional sub-equation method and its applications to nonlinear fractional PDEs. *Physics Letters A*, 375(7):1069–1073, 2011.